



## Widespread remagnetizations and a new view of Neogene tectonic rotations within the Australia-Pacific plate boundary zone, New Zealand

Christopher J. Rowan<sup>1,2</sup> and Andrew P. Roberts<sup>1</sup>

Received 23 June 2006; revised 14 August 2007; accepted 14 September 2007; published 19 March 2008.

[1] Large, clockwise, vertical axis tectonic rotations of the Hikurangi margin, East Coast, New Zealand, have been inferred over both geological and contemporary timescales, from paleomagnetic and geodetic data, respectively. Previous interpretations of paleomagnetic data have laterally divided the margin into independently rotating domains; this is not a feature of the short-term velocity field, and it is also difficult to reconcile with the large-scale boundary forces driving the rotation. New paleomagnetic results, rigorously constrained by field tests, demonstrate that late diagenetic growth of the iron sulfide greigite has remagnetized up to 65% of sampled localities on the Hikurangi margin. When these remagnetizations are accounted for, similar rates, magnitudes, and timings of tectonic rotation can be inferred for the entire Hikurangi margin south of the Raukumara Peninsula in the last 7–10 Ma. Numerous large ( $50\text{--}80^\circ$ ) declination anomalies from magnetizations acquired in the late Miocene require much greater rates of rotation ( $8\text{--}14^\circ \text{Ma}^{-1}$ ) than the presently observed rate of  $3\text{--}4^\circ \text{Ma}^{-1}$ , which is only likely to be characteristic of the tectonic regime established since 1–2 Ma. These new results are consistent with both long- and short-term deformation on the Hikurangi margin being driven by realignment of the subducting Pacific plate, with collision of the Hikurangi Plateau in the late Miocene potentially being key to both the initiation of tectonic rotations and the widespread remagnetization of Neogene sediments. However, accommodating faster, more coherent rotation of the Hikurangi margin in Neogene reconstructions of the New Zealand plate boundary region, particularly in the late Miocene, remains a challenge.

**Citation:** Rowan, C. J., and A. P. Roberts (2008), Widespread remagnetizations and a new view of Neogene tectonic rotations within the Australia-Pacific plate boundary zone, New Zealand, *J. Geophys. Res.*, 113, B03103, doi:10.1029/2006JB004594.

### 1. Introduction

[2] The Hikurangi margin, on the East Coast of New Zealand, structurally links the Tonga-Kermadec subduction zone north of New Zealand, with associated slab roll-back and back-arc spreading, to a zone of intracontinental transpression on the South Island of New Zealand, where underthrusting of buoyant continental crust (the Chatham Rise) impedes subduction and transfers interplate motion to the Marlborough and Alpine-Wairau faults (Figure 1a). This transition is associated with subduction of anomalously thick oceanic crust of the Hikurangi Plateau [Davy and Wood, 1994; Wood and Davy, 1994] beneath the East Coast of the North Island.

[3] Vertical axis tectonic rotations are an important feature of crustal deformation in this region, on both decadal

and geological timescales. The short-term velocity field, derived from a combination of geodetic data and Quaternary fault slip rates [e.g., *Beanland et al.*, 1998; *Wallace et al.*, 2004], indicates that the entire fore arc is actively rotating clockwise at  $\sim 3\text{--}4^\circ \text{Ma}^{-1}$  with respect to the Australian plate (Figure 1a). Paleomagnetic studies of tectonically uplifted marine sediments on the eastern North Island and northeastern South Island [Walcott *et al.*, 1981; Walcott and Mumme, 1982; Mumme and Walcott, 1985; Wright and Walcott, 1986; Mumme *et al.*, 1989; Roberts, 1992, 1995a; Vickery and Lamb, 1995; Thornley, 1996; Little and Roberts, 1997] also report large clockwise declination anomalies (Figure 1b), that indicate tectonic rotations have been a long-term feature of deformation on the Hikurangi margin. Declination anomalies of  $30\text{--}40^\circ$  have been reported from late Miocene (6–11 Ma) sediments from the central part of the margin [Wright and Walcott, 1986]; early Miocene sediments from the northeast North Island (Raukumara Peninsula) indicate no tectonic rotation with respect to the Australian plate [Walcott and Mumme, 1982; Mumme *et al.*, 1989; Thornley, 1996]; and sparse data from the southern North Island have been interpreted to indicate late Miocene rotations that had ceased by 2 Ma [Walcott *et*

<sup>1</sup>National Oceanography Centre, University of Southampton, Southampton, UK.

<sup>2</sup>Now at Department of Geology, University of Johannesburg, Johannesburg, South Africa.

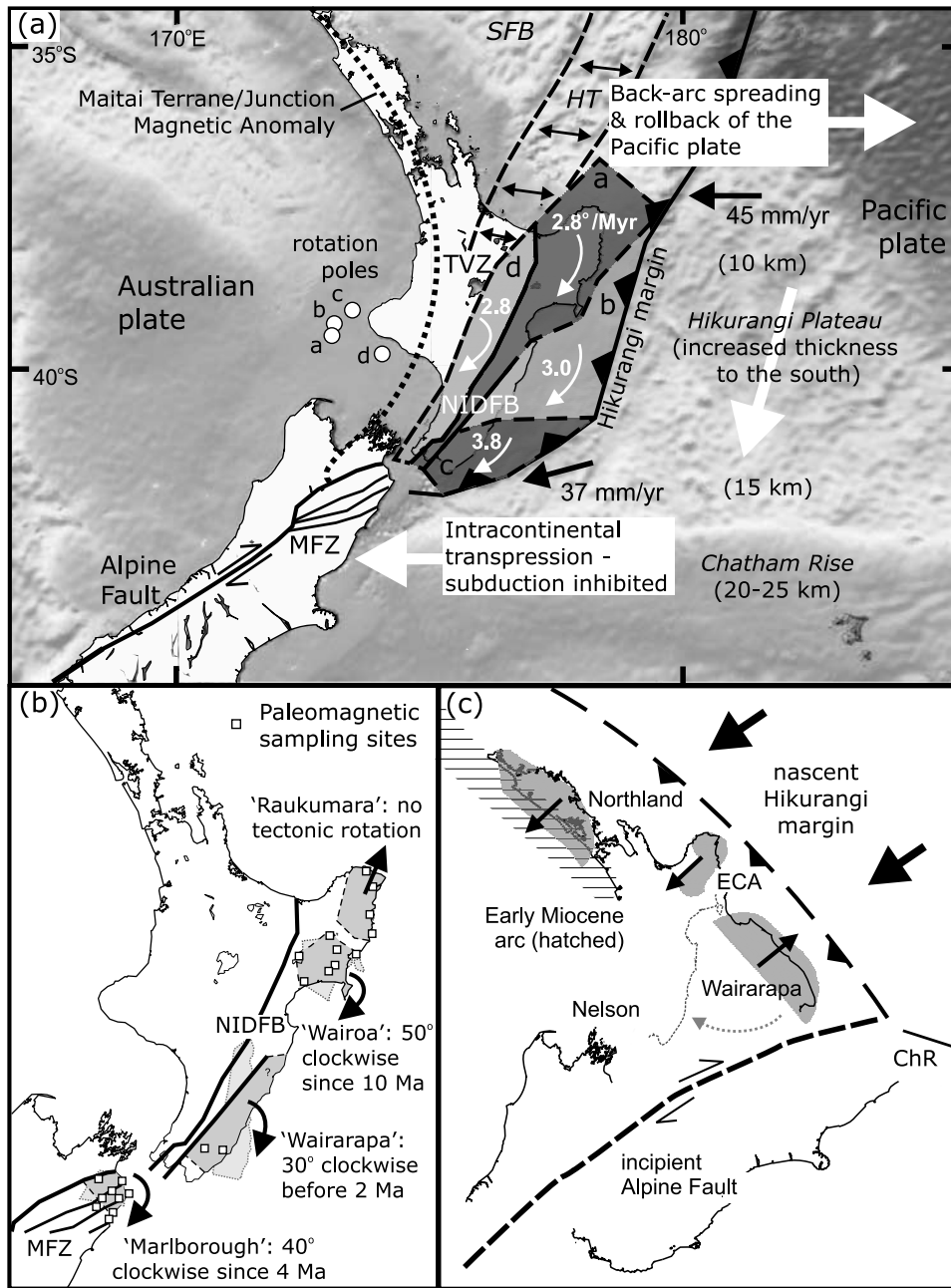


**Figure 1.** (a) Contemporary geodynamics of the New Zealand plate boundary region (bathymetry from *Smith and Sandwell* [1997]). Subduction of thickened oceanic crust (the Hikurangi Plateau) beneath the Hikurangi margin links subduction and back-arc spreading north of New Zealand with intracontinental transpression on the Alpine and Marlborough fault systems; the Hikurangi margin rotates clockwise in response to this transition. The rotating fore arc is divided into a number of separate blocks to account for slip on faults of the North Island Dextral Fault Belt (NIDFB), following *Wallace et al.* [2004]. SFB, South Fiji Basin; HT, Havre Trough; TVZ, Taupo Volcanic Zone; MFZ, Marlborough Fault Zone. (b) Proposed division of the Hikurangi margin into independently rotating “domains” (shaded) based on inferred differences in tectonic rotations recorded by paleomagnetic data (squares) [cf. *Walcott*, 1989]. (c) Reconstruction of the Hikurangi margin at 20–23 Ma, following *Rait et al.* [1991], with early Miocene thrust belts realigned along a NW-SE trending margin that has subsequently rotated up to 90° clockwise. ECA, East Coast Allochthon; ChR, Chatham Rise.

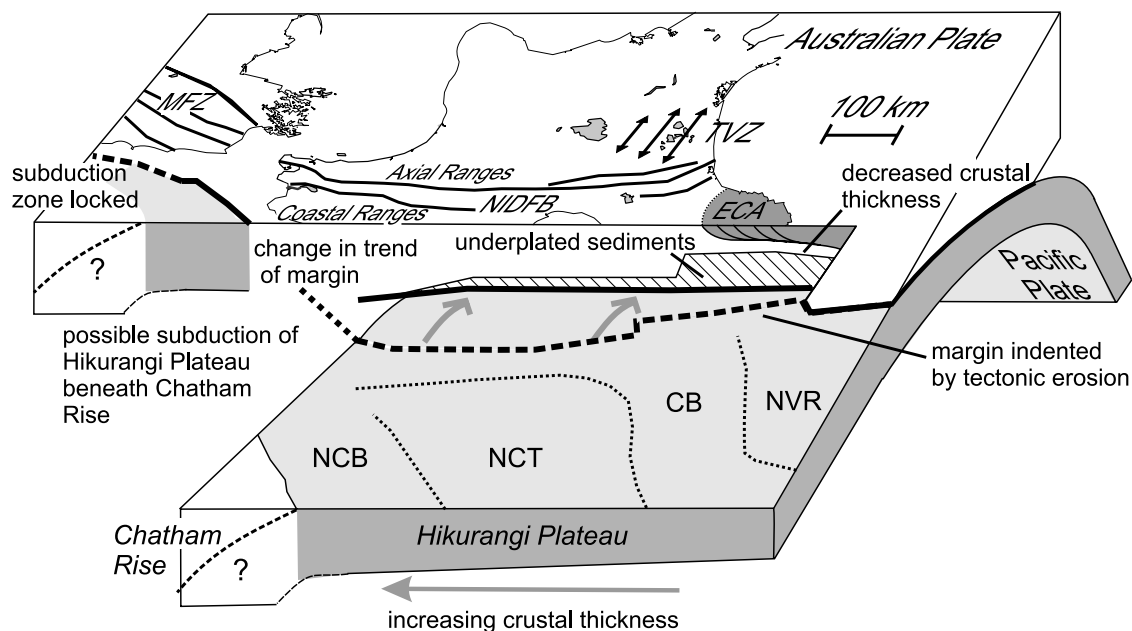


**Figure 2.** N-S cross section along the Hikurangi margin, illustrating lateral variations in the structure of the subducting and overriding plates. Vertical dimensions have been exaggerated for clarity. Dotted lines on the Hikurangi Plateau mark the structural divisions of Wood and Davy [1994] (NVR, Northern Volcanic Region; CB, Central Basin; NCT, North Chatham Terrace; NCB, North Chatham Basin). Other abbreviations are as in Figure 1.

*al.*, 1981; Lamb, 1988]. In the Marlborough region (northeast South Island), two distinct periods of rotation, in the early Miocene and from the early Pliocene (circa 4 Ma) onward, have been observed [Walcott *et al.*, 1981; Lamb, 1988; Roberts, 1992, 1995a; Vickery and Lamb, 1995; Little and Roberts, 1997; Hall *et al.*, 2004]. These observations led to the proposal that the margin is divided into discrete, fault-bounded “domains,” with independent tectonic histories [Lamb, 1988; Walcott, 1989] (Figure 1b). However, aspects of this model are difficult to reconcile with the current geodynamics and structure of the Hikurangi margin. Wallace *et al.* [2004] modeled contemporary deformation using a number of rotating blocks, bounded by major faults of the North Island Dextral Fault Belt (NIDFB) [Beanland, 1995], but these blocks do not correlate to the paleomagnetically defined domains, and they all have similar rates and poles of rotation (Figure 1). Present-day rotation of the margin appears to be linked to a gradual southward increase in the thickness of the subducting Hikurangi Plateau, from 10 to 15 km [Davy and Wood, 1994] (Figures 1a and 2), which gradually increases coupling across the plate interface [Reyners, 1998], and creates a smooth margin-normal shear gradient that is most easily accommodated by bulk clockwise rotation of the entire margin [Walcott, 1989; Wallace *et al.*, 2004]. The domain model suggests much smaller-scale variation of the forces driving rotation, and structures capable of accommodating large differential rotations between adjacent blocks are not readily apparent in either the surface or subsurface geology. Postulated “tears” in the subducting plate [Reyners, 1983; Smith *et al.*, 1989], thought to correlate to the boundaries of the paleomagnetic domains, have since been ruled out by high-resolution surveys of seismicity along the plate boundary [Ansell and Bannister, 1996] (Figure 2).

[4] Prior to the development of key features of the current tectonic regime, including the NIDFB and the Taupo Volcanic Zone (TVZ), since 1–2 Ma [Beanland, 1995; Wilson *et al.*, 1995; Beanland *et al.*, 1998], different structures must have been involved in accommodating interplate motion. The mismatch between paleomagnetically and geodetically determined rotations may therefore be a consequence of the ongoing evolution of structures in the New Zealand plate boundary zone. However, reconciling paleomagnetic with other geological data has still proven difficult, with numerous alternative reconstructions being proposed [King, 2000, and references therein]. At the other extreme from the domain model, the large disparity between the southwestward transport directions of the Northland and East Coast allochthons [Stoneley, 1968; Spörli, 1982; Rait, 2000], which were obducted in the late Oligocene–early Miocene (20–25 Ma) [Rait *et al.*, 1991], and the northeastward shortening direction recorded by the coeval Wairarapa thrust belt [Chanier and Ferrière, 1989], have been cited as evidence that the entire Hikurangi margin south of the Raukumara Peninsula has coherently rotated up to 90° clockwise since the early Miocene [Rait *et al.*, 1991], prior to which it shared the northwest-southeast trend of the early Miocene Northland arc [Herzer, 1995] (Figure 1c). However, this model requires several hundred kilometers of Neogene shortening in the southern North Island, which appears to be inconsistent with fault displacements in the southern fore arc [Nicol and Beavan, 2003] and the low metamorphic grade of rocks in this region [Field *et al.*, 1997].

[5] These difficulties may, in part, be due to problems with existing paleomagnetic data. The strong present-day field (PDF) overprints common in this region were often not completely removed by the blanket demagnetization tech-

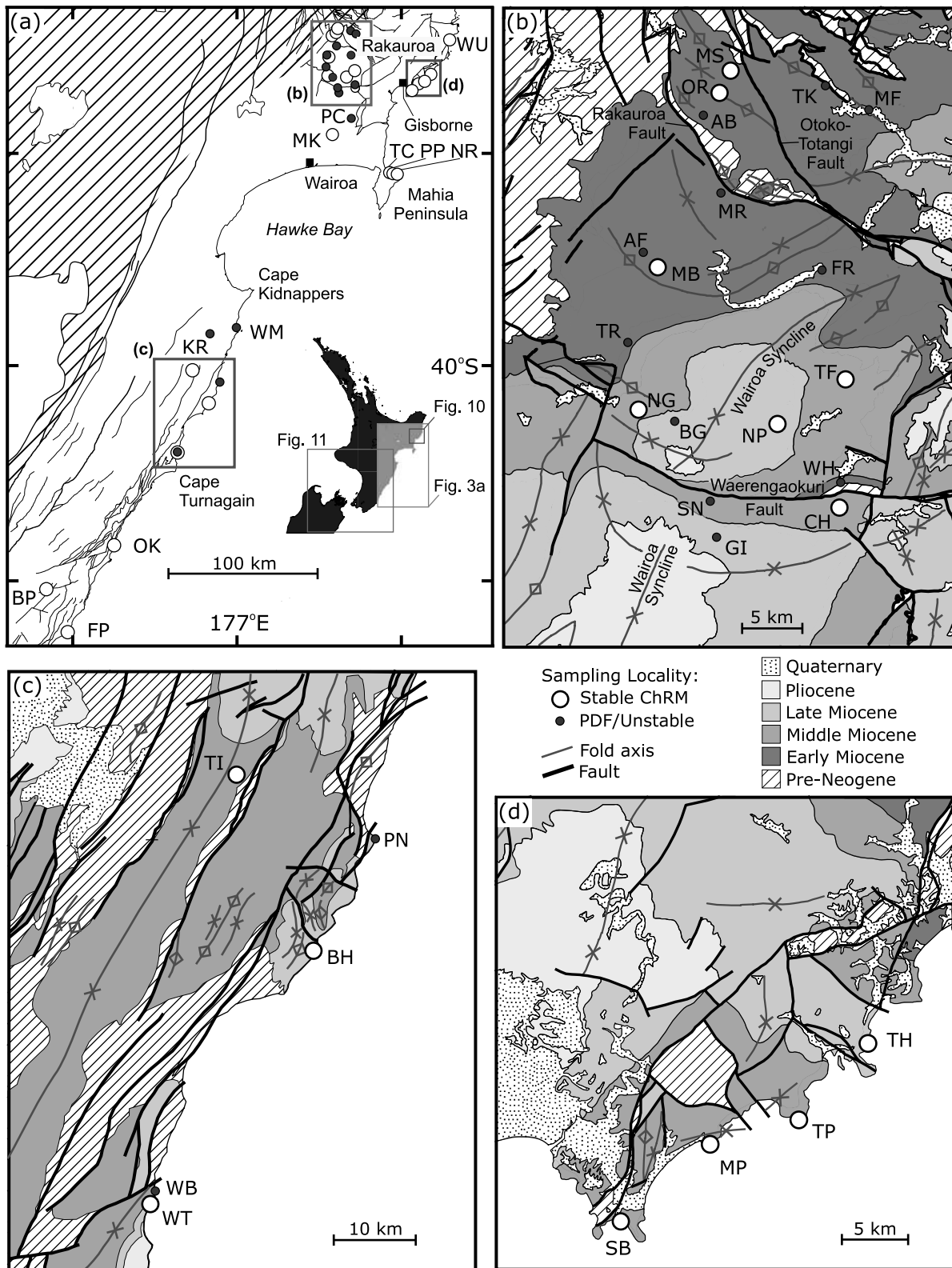


**Figure 3.** Distribution of sampling localities on the Hikurangi margin. Densely sampled areas in (b) the Wairoa Syncline and environs, (c) Southern Hawke Bay, and (d) the coastal region between Gisborne and Tolaga Bay (pre-Neogene outcrop in this area is the result of smectite diapirism), are enlarged to show more detail. Full locality names are given in Table 1; Figures 3a, 3b, and 3d use information from the QMAP data set [Mazengarb and Speden, 2000; Lee and Begg, 2002]; Figure 3c is modified from Kingma [1962].

**Table 1.** Location and Geological Details of Sampling Localities in This Study<sup>a</sup>

Locality	Grid Reference	Age, Ma	Principal Lithology	Average Bedding	Sampled Section	Paleomagnetic Behavior
<i>Rakaurua (Figure 3b)</i>						
MB Mokonui Bridge	X17/074860	16.8 ± 0.8	dark, calcareous mud/siltstones	027/18 SE	33 m	S
MS Matawai Station <sup>b</sup>	X17/128009	20.4 ± 1.4	blue-grey mudstones, sandstones	088/54 S	47 m	SO
OR Oliver Road <sup>b</sup>	X17/118988	20.4 ± 1.4	grey and brown sandy mud/siltstones	067/12 SE	27 m	SO
MR Makaretu Road	X17/118917	17.5 ± 1.5	fine blue-grey sandstones	086/30 S	11 m	U
FR Falkner Road	X17/191864	16.8 ± 0.8	sand-rich siltstones	105/29 S	3 m	PDF
AF Atea Ford	X17/063871	16.8 ± 0.8	sand-rich mudstones, sandstones	017/12 E	41 m	PDF
TK Te Koawa	X17/196994	17.5 ± 1.5	light grey calcareous mudstones	309/56 NE	46 m	PDF
AB Anzac Bridge <sup>b</sup>	X17/096972	20.4 ± 1.6	massive blue-grey mudstones	298/57 NE	53 m	PDF
MF Maharahara Farm	X17/223976	20.4 ± 1.6	mudstones and fine sandstones	090/32 S	22 m	PDF
<i>Wairoa Syncline (Figure 3b)</i>						
MK Mangapoike River	X19/071449	6 ± 1	massive, light grey mudstones	187/30 W	16 m	S
NP Ngatara-Poha	X18/160749	9.9 ± 1.1	sand-rich mudstones, sandstones	186/23 W	82 m <sup>c</sup>	S
TF Te Korau Farm	X18/205761	13.1 ± 2.1	dark, sandy mud/siltstones	199/20 W	13 m	S
NG Ngatimita	X18/063762	13.5 ± 2.5	mud/siltstones and sandstones	084/43 S	21 m	SO
CH Cheviot Hills	X18/204688	14.2 ± 1	mudstones and sand-rich mudstones	072/56 S	17 m	SO
PC Paparatu Cottage	X18/175529	15.6 ± 0.5	mud/siltstones and fine sandstones	183/21 W	19 m	SO
GI Glen Innes	X18/116668	7.6 ± 1.1	sand-rich siltstones, sandstones	085/44 S	19 m	PDF
BG Burgess Road <sup>c</sup>	X18/088752	9.9 ± 1.1	sand-rich mudstones	064/42 SE	14 m	PDF
SN Strathblane Farm	X18/111696	14.2 ± 1	brown mud/siltstones and sandstones	146/27 SW	25 m	PDF
TR Taumata Road	X17/053807	15.6 ± 0.5	massive grey mud/siltstones	348/19 E	47 m	PDF
WH Waterfall Hill <sup>c</sup>	X18/204706	21.4 ± 1.2	mudstones and massive sandstones	238/63 NW	28 m	PDF
<i>Coast North of Gisborne (Figure 3d)</i>						
TH Turihau Point	Y18/608739	8.8 ± 2.3	massive, dark grey mudstones	038/19 SE	14 m	S
WU Waihau Beach <sup>d</sup>	Z17/719916	9.9 ± 1.1	massive grey mudstones and tuffs	194/23 W	7 m	S
MP Makarori Point	Y18/541693	14.6 ± 1.4	turbidites with blue-grey pelagic interbeds	307/14 NE	10 m	S
TP Tatapouri Point	Y18/574705	14.6 ± 1.4	turbidites with blue-grey pelagic interbeds	273/32 N	19 m	S
SB Sponge Bay	Y18/498658	14.6 ± 1.4	turbidites with blue-grey pelagic interbeds	353/47 E	43 m	SO
<i>Mahia Peninsula (Figure 3a)</i>						
TC Te Waipera Cemetery <sup>c</sup>	Y19/362233	7.6 ± 1.1	dark mudstones and tuff beds	203/10 NW	24 m	S
PP Putiki Point <sup>c</sup>	Y19/379226	7.6 ± 1.1	white, ash-rich mudstones	239/11 NW	17 m	SO
NR Nukutaurua Road <sup>c</sup>	Y19/402222	8.8 ± 2.3	pale grey mudstones and reworked tuffs	240/48 NW	82 m	S
<i>Southern Hawke Bay (Figure 3c)</i>						
BH Blackhead	V23/359074	8.8 ± 2.3	massive light grey mud/siltstones	067/23 SE	13 m	SO
WT Whangaehu Tuff	V24/186826	8.8 ± 2.3	tuff bed within sand-rich siltstones	051/38 SE	10 m	SO
TI Titoki Road	V23/281249	14.2 ± 1	brown and grey mud/siltstones	201/30 W	23 m	S
PN Paoanui Point	V23/420182	12.1 ± 1.1	dark, blue-grey mudstones	033/61 SE	47 m	PDF
WB Whangaehu Beach	V24/185829	12.1 ± 1.1	black and grey mudstones	054/73 SE	44 m	PDF
KR Kahuranaki Road	V22/380435	13.5 ± 2.5	mudstones, fine siltstones, sandstones	196/65 W	32 m	U
WM Waimarama Beach	W22/519461	22.1 ± 3.1	light blue grey mudstones, welded tuffs	285/46 N	13 m	PDF
<i>South Wairarapa (Figure 3a)</i>						
BP Brancepeth	T26/485148	8.8 ± 2.3	light grey calcareous mudstones	229/18 NW	35 m	SO
FP Flat Point	T27/587925	19.6 ± 2.1	blue-grey mudstones, glauconitic sands	223/41 NW	14 m	SO
OK Okau	U26/840361	21.9 ± 1.6	fine-grained turbidites	207/50 W	22 m	S

<sup>a</sup>Grid references are from NZMS 260 sheets. Bedding measurements are given as strike and dip with dip direction. Demagnetization behavior is classified as follows: S, stable ChRM with negligible overprint; SO, ChRM strongly overprinted by present-day field but still recoverable; PDF, no ChRM evident beneath present-day field component; U, magnetization difficult to interpret.

<sup>b</sup>Data from these localities are presented fully by Rowan *et al.* [2005].

<sup>c</sup>Data from these localities are presented fully by Rowan and Roberts [2006].

<sup>d</sup>Data from this locality are presented fully by Rowan and Roberts [2005].

<sup>e</sup>Sampling at NP was in two 6–7 m sections separated by an interval with no exposure.

niques frequently used in early studies [Rowan *et al.*, 2005]. More significantly, the magnetization of New Zealand Neogene marine sediments is commonly carried by the authigenic iron sulfide, greigite (Fe<sub>3</sub>S<sub>4</sub>) [Roberts and Turner, 1993; Rowan and Roberts, 2005, 2006]. Numerous studies have shown that where greigite is present, remanence acquisition can occur during late diagenesis, potentially several million years after deposition [e.g., Florindo and Sagnotti, 1995; Horng *et al.*, 1998; Jiang *et al.*, 2001; Roberts and Weaver, 2005; Rowan and Roberts, 2005, 2006; Sagnotti *et*

*al.*, 2005]. Difficulties in extracting a reliable paleomagnetic signal from weakly magnetized New Zealand mudstones mean that good constraints on the timing of remanence acquisition from field tests are usually lacking in published data from the Hikurangi margin; late remagnetizations may therefore have gone unrecognized, leading to a loss of information regarding tectonic rotations.

[6] We present a major new paleomagnetic data set from the East Coast of the North Island, New Zealand. We demonstrate that at sites where the timing of remanence

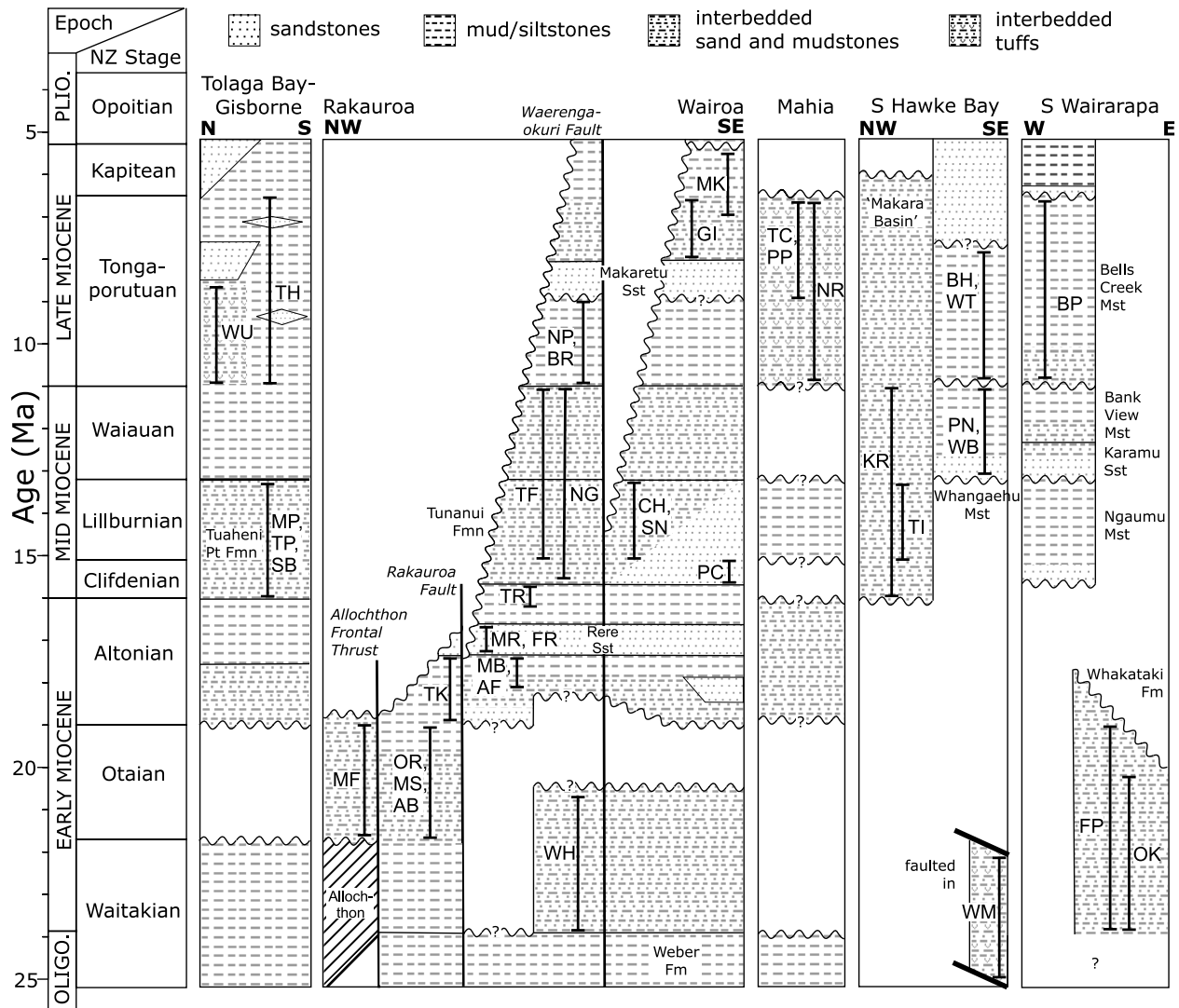


Figure 4. Generalized stratigraphy of the East Coast region, indicating the stratigraphic ranges of the sampling localities listed in Table 1. Adapted from *Field et al.* [1997] with additional information from *Neef* [1992], *Davies et al.* [2000], *Mazengarb and Speden* [2000], and *Francis et al.* [2004].

acquisition can be properly constrained by structural field tests, the magnetization often postdates deposition by several million years. Recognition of widespread remagnetizations results in a substantially modified history of Neogene tectonic rotations on the Hikurangi margin.

**2. Sample Collection and Paleomagnetic Analysis**

[7] Standard (25 mm diameter) paleomagnetic cores were collected from 38 localities distributed along the Hikurangi margin (Figure 3a and Table 1). The approximate stratigraphic intervals sampled at these localities are shown on generalized stratigraphic columns in Figure 4. Fine-grained sedimentary sequences with unambiguous and consistent bedding orientation were targeted in all cases. Continuous exposures of >10 m of section were preferred to ensure that the effects of geomagnetic secular variation were properly averaged. To minimize viscous magnetic overprints, weathered surficial material was removed from the outcrop prior

to sampling, and, upon retrieval, cores were immediately placed in a mu-metal shield. Cores were cut into samples of 21 mm length; paleomagnetic measurements were then made using a 2G-Enterprises cryogenic magnetometer (sensitivity of  $\sim 10^{-12}$  A m<sup>2</sup>), situated in a magnetically shielded laboratory at the National Oceanography Centre, Southampton (NOCS). Both thermal (40° steps from 80°C to 400°C) and alternating field (AF) (5 mT steps to 60 mT) demagnetization techniques were used; low-field bulk magnetic susceptibility was measured for thermally demagnetized samples after each heating step to monitor for thermal alteration.

[8] Characteristic remanent magnetization (ChRM) directions were calculated using principal component analysis of stepwise demagnetization data [*Kirschvink*, 1980]. Mean directions and confidence limits for stably magnetized localities were calculated according to *Fisher* [1953]. If great circle demagnetization paths were observed at localities where strong overprints were prevalent, they were used to better constrain the mean direction [*McFadden and*

*McElhinny*, 1988]. Where localities of similar age were distributed across well-defined structures, a fold test [*Tauxe and Watson*, 1994] was applied to ChRM data to constrain the timing of remanence acquisition.

### 3. Results

#### 3.1. Demagnetization Behavior

[9] Rock magnetic and scanning electron microscope observations of the studied sediments [*Rowan and Roberts*, 2005, 2006] indicate that they commonly contain variable mixtures of single domain and superparamagnetic greigite, which grew authigenically within the sediments at various stages of diagenesis. Thermal demagnetization behavior, including unblocking at 250–350°C and the onset of thermal alteration (indicated by large increases in low-field bulk magnetic susceptibility) above 350°C, is also consistent with the presence of greigite in many of our samples [cf. *Roberts*, 1995b]. The natural remanent magnetization (NRM) of all samples was weak (typically  $<10^{-4}$  A m<sup>-1</sup>). In geographic coordinates, a PDF overprint (declination (D) = 20°, inclination (I) = -64°) was also commonly observed. This overprint can be linked to pyrite oxidation that is probably associated with modern groundwater percolation [*Rowan and Roberts*, 2006], and its variable strength exerts a major control on demagnetization behavior, which fell into three main classes (Figure 5 and Table 1):

[10] 1. Class S behavior was observed at 12 of the 38 studied localities (33%). The viscous overprint is weak and is removed at low temperatures (<150°C) and AFs (<20 mT), allowing a stable ChRM to be easily isolated (Figures 5a and 5b). At many of these localities, both AF and thermal demagnetization appear to be equally effective at isolating the ChRM.

[11] 2. Class SO behavior was observed at 11 further localities (29%). The viscous overprint is much stronger, and AF demagnetization was generally ineffective, as has often been the case for New Zealand Cenozoic sediments [*Turner et al.*, 1989; *Pillans et al.*, 1994; *Roberts et al.*, 1994; *Turner*, 2001]. Thermal demagnetization data often follow great circle paths toward the ChRM (Figures 5c and 5d), although in many cases a stable end point is not reached (e.g., Figure 5d).

[12] 3. Class PDF behavior was observed at 13 localities (34%). No ChRM appears to be present; progressive removal of the PDF overprint reveals no stable component at higher temperatures or at higher applied fields (Figures 5e and 5f). At these sites, pervasive iron sulfide oxidation has evidently destroyed any ancient magnetization.

[13] Demagnetization data for two remaining localities (4%; class U, uncertain, in Table 1) proved difficult to

interpret, having no obvious PDF overprint and anomalous ChRM directions with shallow inclinations.

#### 3.2. Mean Paleomagnetic Directions

[14] Mean paleomagnetic directions for type S and SO localities are listed in both geographic and tilt-corrected coordinates in Table 2; tilt-corrected ChRM data for these localities, along with representative great circle demagnetization paths where appropriate, are plotted in Figure 6. The reliability of the mean directions calculated for some type SO localities may be questionable due to the small amount of data available, which makes it difficult to assess whether the strong PDF overprint has been completely removed (e.g., FP, PC; see also discussion by *Rowan et al.* [2005]).

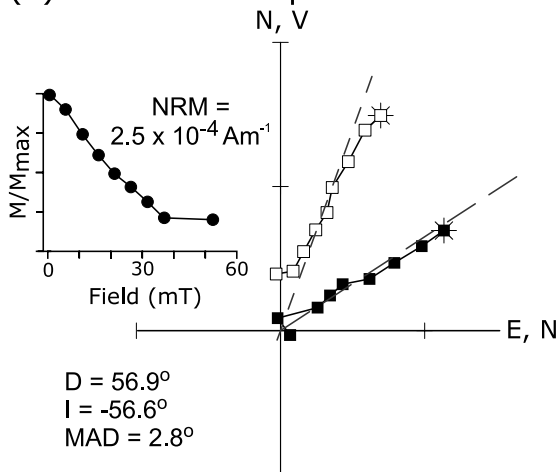
[15] Paleomagnetic declinations (from tilt-corrected mean directions, with errors calculated according to *Demarest* [1983]) are plotted against depositional age for all localities in Figure 7. There is a large amount of scatter in these data, with some of the largest differences in the measured declination (as much as 80°) recorded by sediments of the same age at localities in close proximity to each other (e.g., SB, TP). Additionally, rotations of >80° are recorded by late Miocene sediments, which would require tectonic rotation at substantially higher rates than are presently observed in the short-term velocity field [e.g., *Wallace et al.*, 2004]. However, as stated previously, the assumption that the ChRM dates from the time of deposition is invalid for at least some, and possibly many, of these localities, due to the widespread occurrence of authigenic greigite. In several cases, greigite has formed during late diagenesis, a million years or more after deposition [*Rowan and Roberts*, 2005, 2006]. Taking the declination-age plot in Figure 7 at face value could therefore be highly misleading; rigorous constraints on the timing of magnetization are required to develop a more accurate picture of the rotation history of the Hikurangi margin.

#### 3.3. Constraints on the Timing of Remanence Acquisition

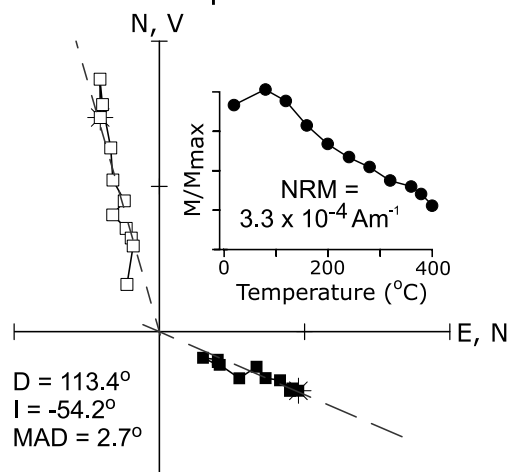
[16] Attempts to establish the age of the ChRM using paleomagnetic field tests, primarily the fold test of *Tauxe and Watson* [1994], was in many cases frustrated by the prevalence of strong PDF overprints, which led to the loss of useful data at critical sites. However, careful analysis of stable magnetizations at neighboring sites, and the local structural context, enables limits to be placed on the timing of remanence acquisition at 16 of the 23 stably magnetized localities, although in some cases these age constraints remain broad (Table 2). Constraints on individual localities are discussed in more detail in sections 3.3.1 and 3.3.2, which are subdivided according to their position on the

**Figure 5.** Vector component plots of representative AF and thermal demagnetization behavior. Solid symbols denote declinations, open symbols denote inclinations, and dashed lines indicate best fit directions from principal component analysis. Demagnetization behavior is subdivided according to the variable strength of the PDF overprint. Class S samples (Figures 5a and 5b) have a stable ChRM with a weak viscous overprint. Class SO samples (Figures 5c and 5d) have a much stronger PDF overprint that overlaps the ChRM, resulting in great circle demagnetization paths (see inset equal-area stereoplots; solid (open) circles represent data in the lower (upper) hemisphere) and sometimes preventing isolation of a stable end point (e.g., Figure 5d). Class PDF samples (Figures 5e and 5f) are also strongly overprinted, but there is no sign of an underlying ChRM. Data are plotted in tilt-corrected coordinates for Figures 5a–5d and in geographic coordinates for Figures 5e–5f.

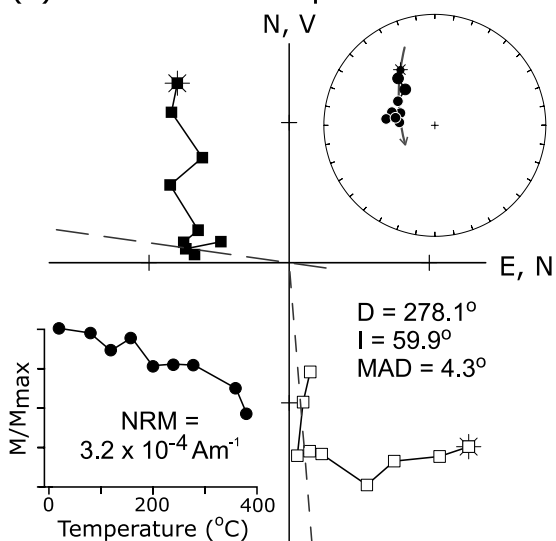
(a) Class S - Sample MK14A



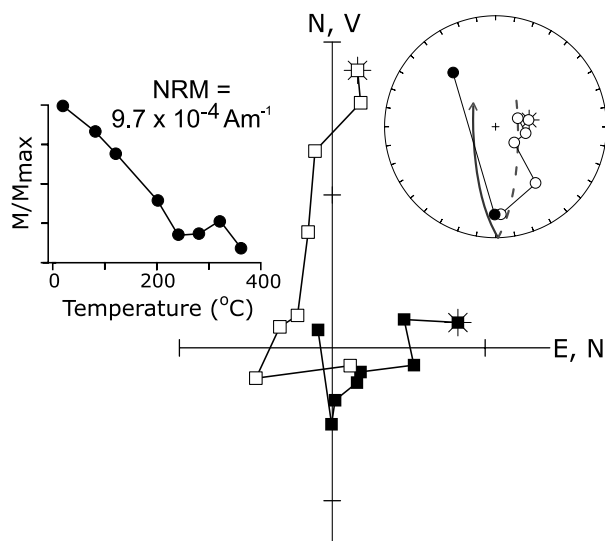
(b) Class S - Sample TP30B



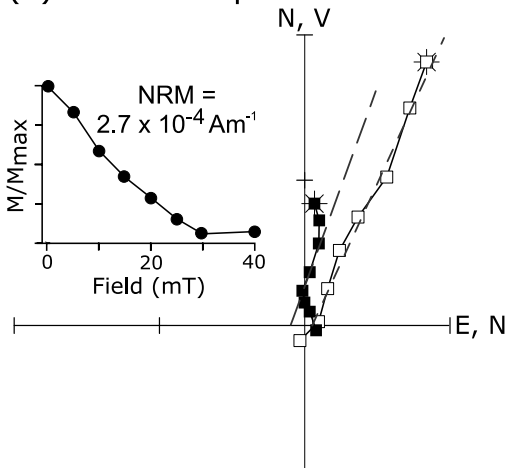
(c) Class SO - Sample CH11B



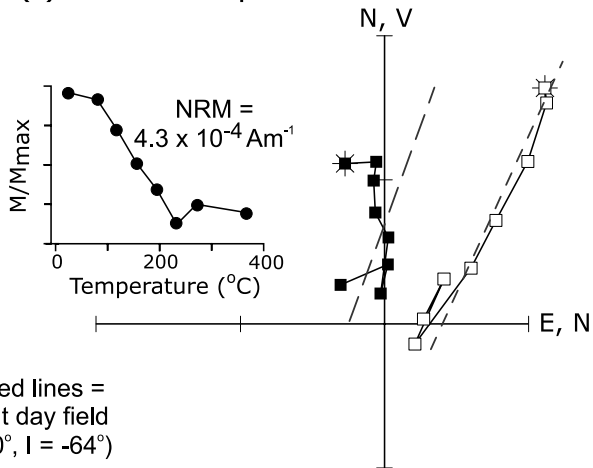
(d) Class SO - Sample BP40A



(e) PDF - Sample PN02A\*



(f) PDF - Sample WM17A\*



\*Dashed lines = present day field ( $D = 20^\circ, I = -64^\circ$ )

Figure 5

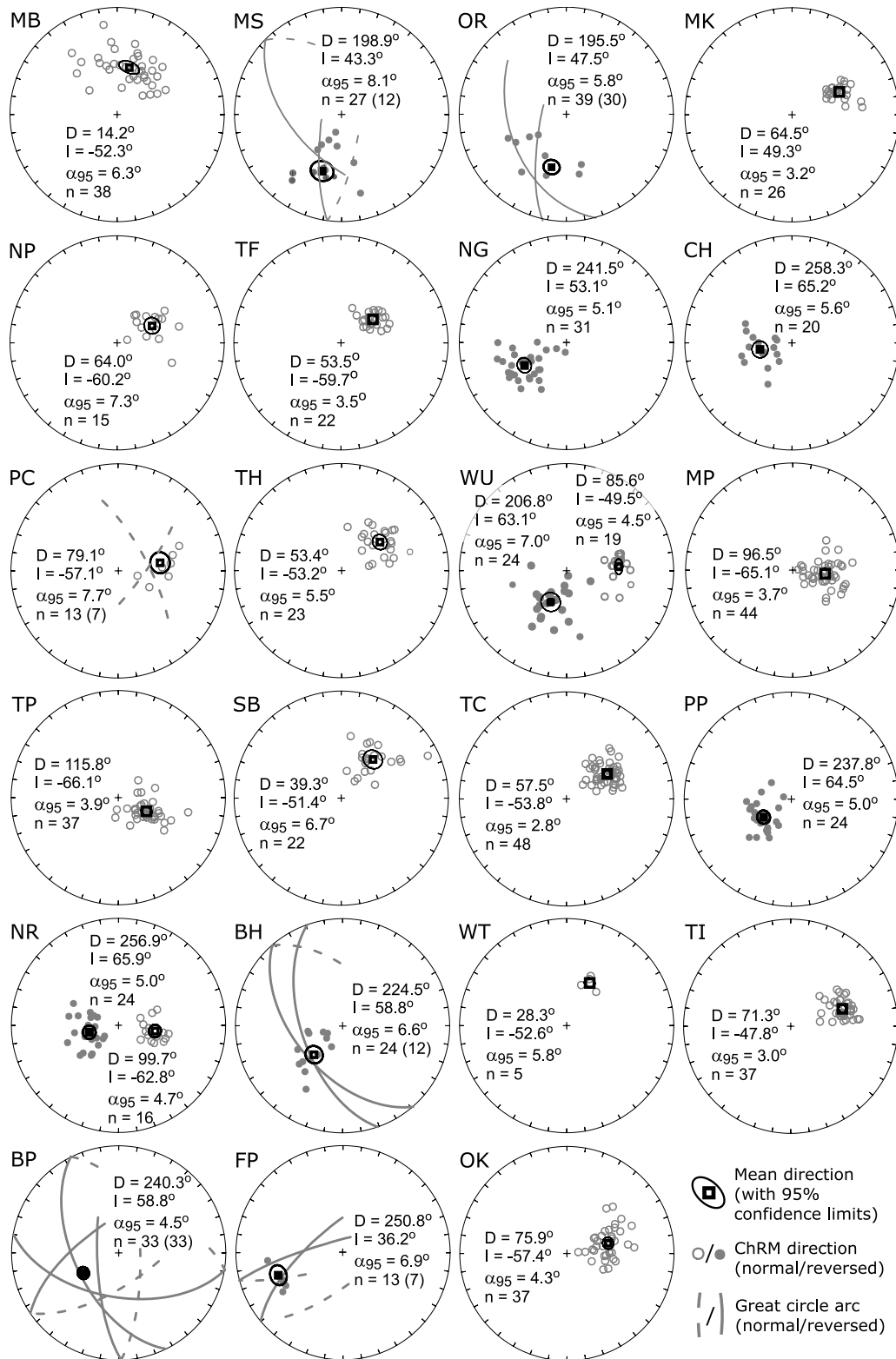


**Figure 6.** Equal-area stereographic plots of tilt-corrected ChRM directions, and mean directions with 95% confidence limits, for all localities in this study where a stable magnetization was isolated. Solid (open) circles represent data plotted in the lower (upper) hemisphere; n is the number of samples used for the calculation; the number in parentheses, if present, records the number of great circle demagnetization paths that were used to constrain the mean direction (representative great circles are plotted for localities where they were used).

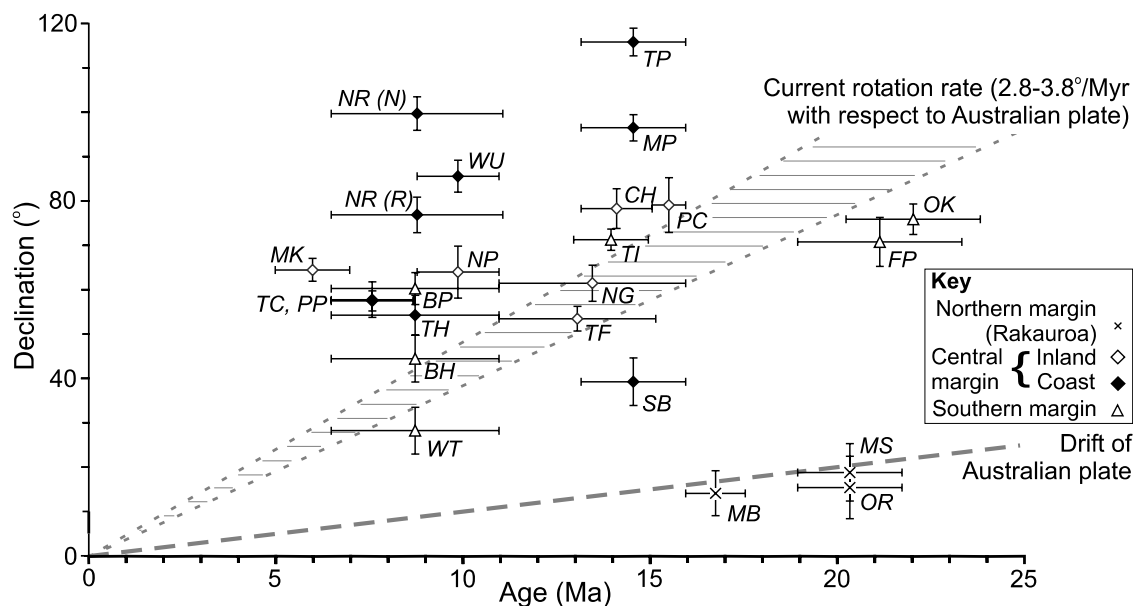


**Figure 7.** Tilt-corrected declinations plotted against depositional age at all localities where a stable ChRM was isolated. Localities have been subdivided according to their position on the margin; the northern, central, and southern Hikurangi margin are roughly equivalent to the Raukumara, Wairoa, and Wairarapa domains of *Walcott* [1989].

Hikurangi margin; the “central” and “southern” regions are roughly equivalent to the Wairoa and Wairarapa domains of *Walcott* [1989] (Figure 1b).

### 3.3.1. Central Margin

#### 3.3.1.1. Rakauroa Region

[17] Reversed polarity magnetizations in early Miocene (Otaian) sediments at Oliver Road (OR) and Matawai Station (MS) (Figure 3b) predate early Miocene (Altonian) folding [Rowan *et al.*, 2005]. The small declinations observed ( $<20^\circ$ ; Figure 6) are consistent with expected values for the Australian plate [Idnurm, 1985] (Figure 7), indicating negligible Neogene tectonic rotations in this area. This contrasts with the large declination anomaly reported from this region by *Mumme and Walcott* [1985], which resulted from incomplete removal of a PDF overprint [Rowan *et al.*, 2005]. Many other localities sampled in this area were also compromised by strong PDF overprints (Table 1). A stable ChRM was isolated from early Miocene sediments at Mokonui Bridge (MB) (Figures 3b and 6), but the timing of the magnetization cannot be constrained in this case.

#### 3.3.1.2. Wairoa Syncline

[18] Many localities distributed across the Wairoa Syncline, to the south of Rakauroa (Figure 3b), were also affected by strong PDF overprints, which often obscured the primary paleomagnetic signal (Table 1). Of the six localities from which a stable ChRM was retrieved, no constraints could be placed on the timing of magnetization at Ngatarā-Poha (NP), Papatatu Cottage (PC) and Mangapoike River (MK); mean declinations and inclinations from these localities are plausible both before and after tilt correction (Table 2). Only results from Te Korau Farm (TF) and Ngatimita (NG) could be subjected to a fold test, which indicates that remanence acquisition occurred before folding of the Wairoa Syncline (Figures 8a and 8b). These localities yielded tilt-corrected declinations of  $54 \pm 2^\circ$  and

$62 \pm 4^\circ$ , respectively (Figure 6). South of the Waerengaokuri Fault, a large, reversed polarity declination of  $78 \pm 5^\circ$  at Cheviot Hills (CH) also appears to record a prefolding magnetization: in geographic coordinates the mean direction is unrealistic, with a large declination requiring  $140^\circ$  of tectonic rotation, and a shallow inclination (Figure 8a and Table 2). Unfortunately, at all of these localities a large time window exists between deposition in the middle Miocene and folding from the Pliocene onward [Field *et al.*, 1997], meaning that constraints on the age of their magnetizations remain broad. Declinations at TF and NG are  $20^\circ$  smaller than at CH (Table 2), which may indicate later and earlier forming magnetizations, respectively; this discrepancy could also be due to differential rotations across the Waerengaokuri Fault, but there is no indication that this structure has substantially altered the trend of the earlier-forming Wairoa Syncline, as would be expected if this was the case (Figure 3b).

#### 3.3.1.3. Coast

[19] Coastal sampling between Mahia Peninsula and Tolaga Bay (Figures 3a and 3d) proved particularly successful, with most localities having easily removed PDF overprints and stable paleomagnetic directions (Tables 1 and 2). However, remagnetizations are common. Fold tests indicate that the normal and reversed polarity magnetizations recorded in a late Miocene sequence on Mahia Peninsula (localities TC, PP, NR; Figures 3a and 6) were acquired during folding at 4–6 Ma; the reversed polarity magnetization was acquired demonstrably earlier than the normal polarity magnetization (at 79% and 44% unfolding, respectively [Rowan and Roberts, 2006]). After a partial fold correction, ChRMs from these localities combine to give a mean declination of  $49 \pm 5^\circ$  at 4–6 Ma.

[20] Further to the north, two differently timed magnetizations with opposite polarity have also been recorded in

**Table 2.** Paleomagnetic Mean Directions and Constraints on the Timing of Remanence Acquisition<sup>a</sup>

Locality (Behavior)	n	Mean Directions				Timing of Remanence Acquisition				Corrected Declination	
		Geographic		Tilt-Corrected		Constraint	Untilting	Age, Ma			
		D, deg	I, deg	D, deg	I, deg					$\alpha_{95}$	k
<i>Central Hikurangi Margin (Rakaurao)</i>											
MB (S)	38	37.9	-52.4	14.2	-52.3	6.3	14.5		no constraint		
MS (SO)	27 <sup>(12)</sup>	298.0	72.0	198.9	43.3	8.1	12.6	before early Miocene	100%	19.0–21.7	18.9 ± 6.5°
OR (SO)	39 <sup>(30)</sup>	206.1	56.2	195.5	47.5	5.8	16.3	folding	100%	19.0–21.7	15.5 ± 4.7°
<i>Central Hikurangi Margin (Wairoa Syncline)</i>											
MK (S)	26	21.8	-63.8	64.5	-49.3	3.2	79.6		no constraint		
NP (S)	15	16.5	-74.5	64.0	-60.2	7.3	28.4		no constraint		
TF (S)	22	15.3	-65.5	53.5	-59.7	3.5	80.0	before Pliocene folding	100%	5.0–15.2	53.5 ± 2.4°
NG (SO)	31	297.9	47.6	241.5	53.1	5.1	26.4		100%	5.0–16.0	61.5 ± 4.1°
CH (SO)	20	313.4	27.8	258.3	65.2	5.6	35.3	probably before Pliocene folding	100%	5.0–15.2	78.3 ± 4.5°
PC (SO)	13 <sup>(7)</sup>	58.7	-76.6	79.1	-57.1	7.7	31.5		no constraint		
<i>Central Hikurangi Margin (Coast)</i>											
TC (S)	48	44.3	-58.6	57.5	-53.8	2.8	54.1		44%		
NR (S)	16	6.5	-54.5	99.7	-62.8	4.7	63.3	during late Miocene–Pliocene folding	44%	4.0–6.0	49.1 ± 5.4°
	24	182.6	44.6	256.9	65.9	5.0	36.4		79%		
PP (SO)	24	216.1	62.3	237.8	64.5	5.0	36.2		79%		
WU (S)	19	66.8	-70.2	85.6	-49.5	4.5	55.5	early (large declination)	100%	? –11.0	85.6 ± 3.6°
	24	163.9	59.3	206.8	63.1	7.0	18.7	late (small declination)	100%	0.8–?	26.8 ± 5.4°
MP (S)	44	77.2	-56.0	96.5	-65.1	3.7	35.3	between Miocene and Pliocene deformation episodes	0%	3.6–8.8	51.2 ± 2.2°
TP (S)	37	49.8	-59.2	115.8	-66.1	3.9	37.3		0%	3.6–16.0	51.2 ± 2.2°
SB (SO)	22	56.9	-11.7	39.3	-51.4	6.7	22.1	probably before late Miocene–Pliocene diapirism	100%	3.6–16.0	39.3 ± 5.3°
TH (S)	23	73.4	-44.9	53.4	-53.2	5.5	30.7		no constraint		
<i>Southern Hikurangi Margin (Southern Hawke Bay)</i>											
BH (SO)	24 <sup>(12)</sup>	264.6	59.9	224.5	58.8	6.6	21.1	during late Miocene–Pliocene folding			
WT (SO)	5	79.2	-50.1	28.3	-52.6	5.8	176		56%	3.6–8.8	60.2 ± 2.3°
TI (S)	37	31.2	-64.4	71.3	-47.8	3.0	64.6				
<i>Southern Hikurangi Margin (Wairarapa)</i>											
BP (SO)	33 <sup>(33)</sup>	210.6	57.8	240.3	58.8	4.5	32.8		no constraint		
FP (SO)	13 <sup>(7)</sup>	214.6	44.2	250.8	36.2	6.9	36.8		no constraint		
OK (S)	37	339.7	-58.5	75.9	-57.4	4.3	31.2	probably before early Miocene folding	100%	16.0–23.9	75.9 ± 3.4°

<sup>a</sup>Here n is the number of samples; the superscript number indicates the number of great circle arcs used to constrain the mean direction according to *McFadden and McElhinny* [1988]. Errors on corrected declinations are calculated according to *Demarest* [1983].

late Miocene sediments near Tolaga Bay (locality WU, Figure 3a). In this case, however, there is a 60° difference in declination between the mean directions of the reversed and normal polarity magnetizations (Figure 6), which requires several million years of tectonic rotation between their respective acquisition times [Rowan and Roberts, 2005]. The normal polarity magnetization must therefore date from close to the time of deposition and the reversed polarity magnetization was acquired much later, but before the last polarity reversal at 0.78 Ma.

[21] Four other coastal localities were also sampled from middle-late Miocene rocks near Gisborne (Figure 3d), in an area that has undergone at least two separate periods of deformation since the late Miocene. At Tatapouri Point (TP) and Makarori Point (MP), middle Miocene sediments of the Tuaheni Point Formation (Figure 4) [Neef, 1992] have been folded into a syncline, which has then been disrupted by emplacement of a smectite diapir, causing a 20–25° clockwise rotation of the fold axis at MP with respect to TP (Figure 3d). Tilt-corrected paleomagnetic data indicate large (~100°) clockwise declination anomalies at both sites (Figure 6), but the apparent rotation is larger at TP than at MP. With no tilt correction applied, however, the declination

at MP is 27° more rotated than at TP (Table 2 and Figure 8c); this is much more consistent with the structural evidence, and suggests that remanence acquisition at these sites occurred after folding of the syncline, but before emplacement of the diapir. When the data from MP are corrected for a 25° local rotation, a fold test confirms a postfolding remanence (Figure 8d) with a mean declination of 51 ± 2° (Table 2). The first generation of folding also affects late Miocene sediments (Figure 3d), and diapir emplacement occurred in the late Miocene and Pliocene [Neef, 1992; Field *et al.*, 1997]. Remanence acquisition therefore appears to have occurred at the end of the Miocene.

[22] At Sponge Bay (SB), sediments of equivalent age to those sampled at localities MP and TP are steeply tilted as a result of late Miocene–Pliocene diapir emplacement (Figure 3d). This deformation postdates the folding at the other two localities, and therefore a fold test cannot be used to constrain the magnetization age. However, a prefolding remanence appears likely because the mean direction at SB has an unrealistically shallow inclination in geographic coordinates (Figure 8c). The tilt-corrected declination of 39.3 ± 5.3° indicates slightly less rotation than the corrected declination from the MP and TP localities, which suggests,

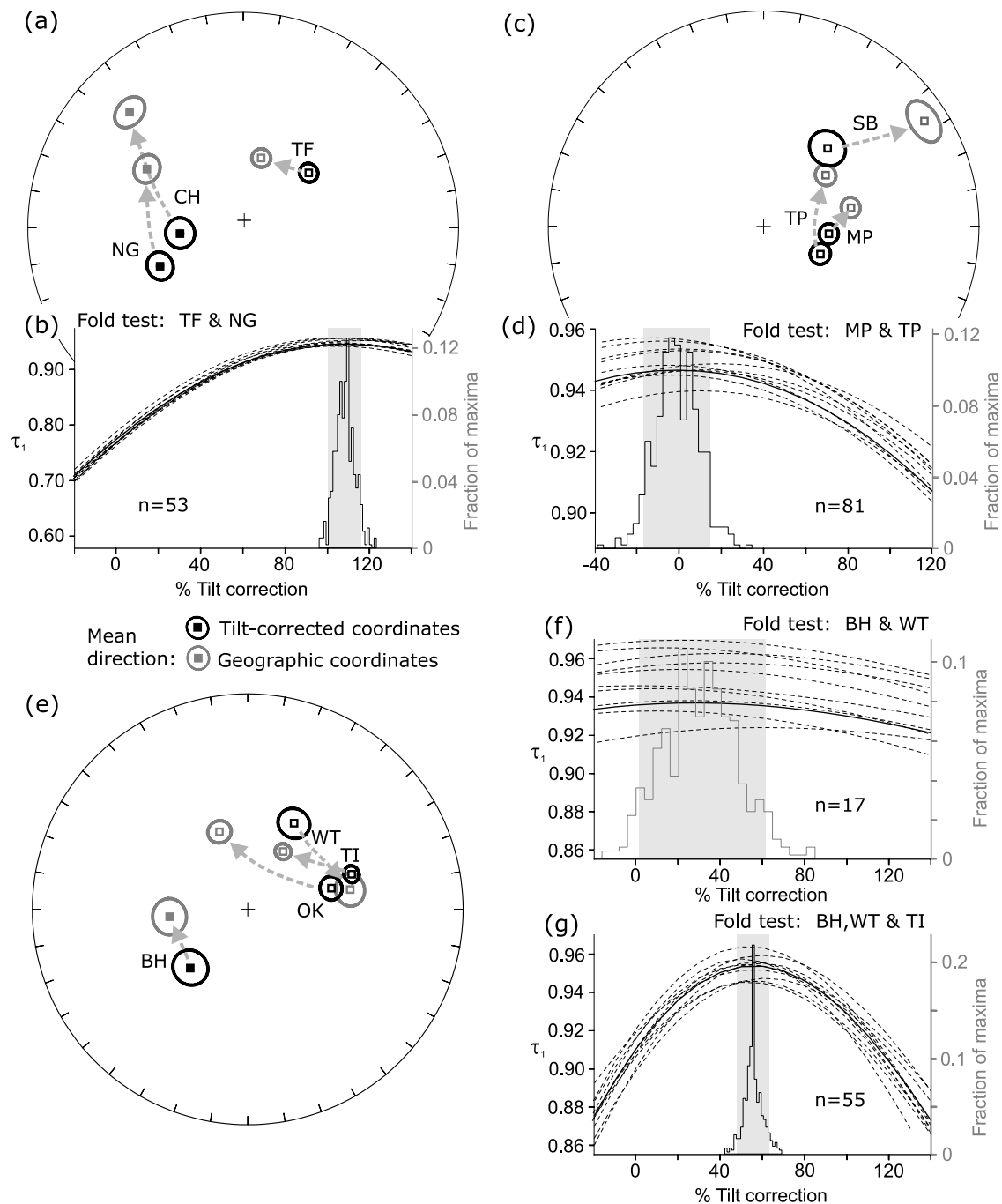


**Figure 8.** Constraints on the timing of remanence acquisition at localities from (a, b) the Wairoa Syncline, (c, d) the coast north of Gisborne, and (e–g) southern Hawke Bay. Stereoplots depict mean directions in tilt-corrected and geographic coordinates. Fold tests follow the method of *Tauxe and Watson* [1994]; variation of the principal eigenvector  $\tau_1$  with various degrees of unfolding is depicted with dashed lines for different para-data sets, the distribution of maxima for these data sets is shown by the histogram, and the grey shading represents the 95% confidence interval.

but does not conclusively demonstrate, a late prefolding remagnetization. In contrast, shallow tilting of late Miocene sediments at Turihaua Point (TH; Figure 3d) cannot be dated with any confidence, so no constraints on remanence acquisition are possible for this locality. A moderate to large

tectonic rotation is indicated in both geographic and tilt-corrected coordinates (Table 2).

### 3.3.2. Southern Margin

#### 3.3.2.1. Southern Hawke Bay

[23] Five coastal localities sampled between Cape Kidnappers and Cape Turnagain (Figures 3a and 3c and Table 1)

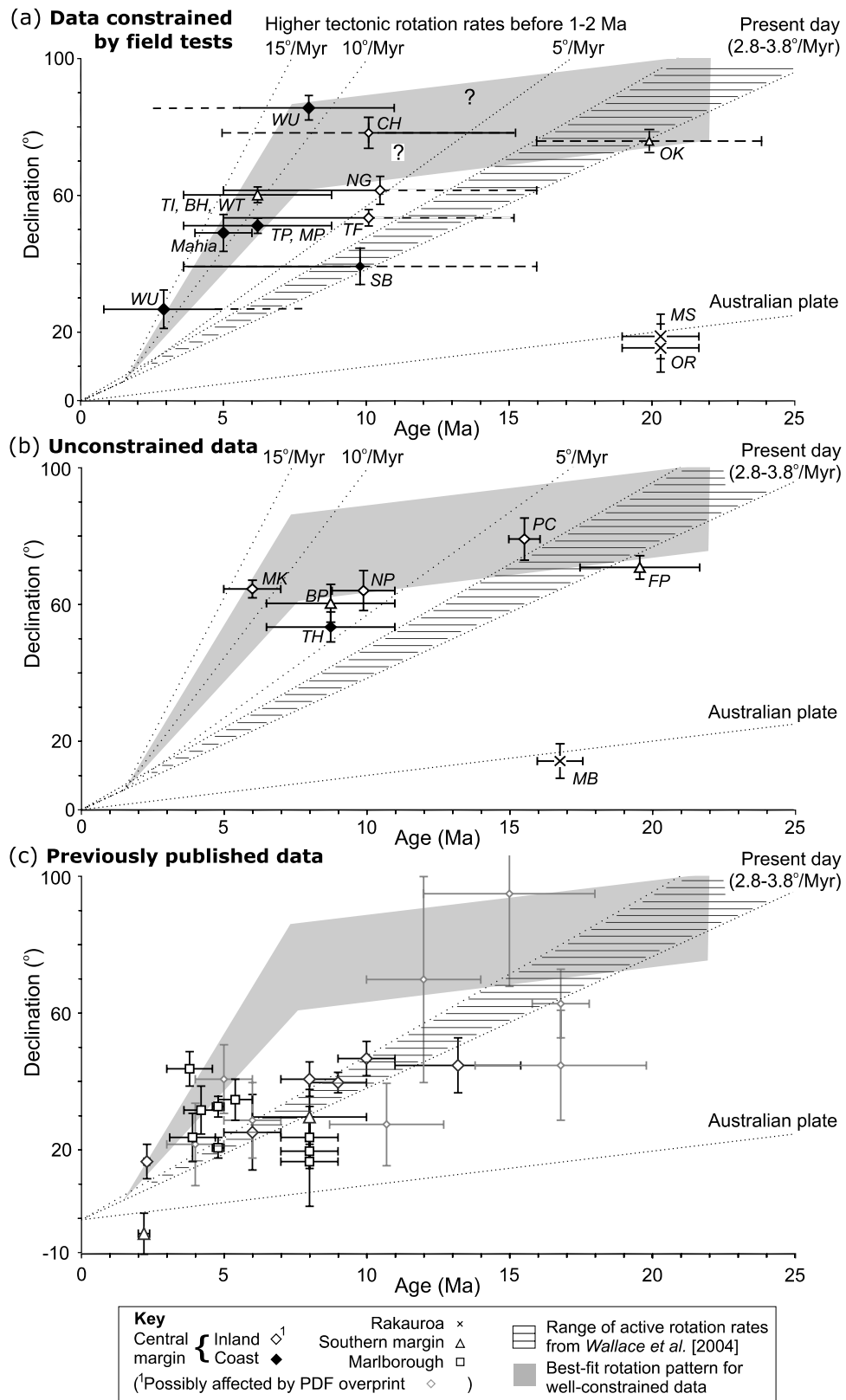


Figure 9

proved to be strongly affected by PDF overprints. Even at the two localities where a stable remanence was isolated, from early late Miocene sediments at Blackhead Beach (BH) and around a tuff horizon of similar age on Whangahau Beach (WT), few samples yielded reliable ChRMs after demagnetization (Figure 6). A fold test indicates a late synfolding magnetization, but the paucity of data, and the similar bedding tilt at these two localities (Table 1) produces a partial tilt correction with a broad 95% confidence interval of 2–62% (Figure 8f).

[24] Much better data were obtained from Titoki Road (TI, Figures 3a and 3c and Table 2). Although these sediments are middle Miocene rather than late Miocene in age, all Miocene strata in this area were folded by the same deformation episode, from the late Miocene–Pliocene onward [Kelsey *et al.*, 1995; Field *et al.*, 1997] (Figure 3c). To test for the presence of a synfolding magnetization at TI, a fold test was performed on the combined ChRM data from TI, BH, and WT. This indicates a synfolding magnetization acquired at 48–63% tilt correction (Figure 8g), which is within the 95% confidence interval of the fold test for BH and WT alone (Figure 8f), but is much better constrained due to the inclusion of additional data from TI. These results suggest a similarly timed synfolding magnetization at all three localities. Applying a partial tilt correction of 56% to the ChRM data from TI, BH, and WT produces a corrected declination of  $60 \pm 2^\circ$  for an assumed magnetization age of 4–9 Ma (Table 2).

### 3.3.2.2. Wairarapa

[25] Three localities were sampled in the Wairarapa region (Figure 3a), two of which were affected by a strong PDF overprint. Few samples from Flat Point (FP), and none from Brancepeth (BP), reached a stable end point on demagnetization. The paleomagnetic mean directions for these two localities therefore rely heavily upon demagnetization great circle data (Figure 6), making these directions potentially unreliable. Furthermore, no ChRM data are available for fold tests to constrain the timing of remanence acquisition. In contrast, at Okau (OK) the PDF overprint was easily removed, allowing a ChRM to be isolated in most samples (Figure 6). The calculated mean direction has an anticlockwise declination anomaly in geographic coordinates (Figure 8e and Table 2), which indicates that the magnetization predates early Miocene (Altonian) folding associated with movement on the nearby Adams-Tinui Fault [Field *et al.*, 1997]. In tilt-corrected coordinates, the paleomagnetic declination is  $76 \pm 3^\circ$  (Figure 6 and Table 2),

which is similar to those obtained from the potentially less reliable FP and BP localities (Figure 6).

## 4. Discussion

### 4.1. Inferred Tectonic Rotations

[26] In order to properly reconstruct Neogene deformation of the Hikurangi margin, the paleomagnetic data set has been reduced to those localities where the timing of remanence acquisition can be reliably constrained, with appropriately corrected declinations for localities with verified synfolding magnetizations (Table 2 and Figure 9a). This reduced data set provides a number of new insights into the pattern of tectonic rotations on the East Coast of New Zealand.

[27] Our data confirm that part of the northern Hikurangi margin has not tectonically rotated over geological time-scales. Although substantial rotations are observed as far north as Tolaga Bay (locality WU) on the coast (Figure 3a), localities further inland (OR and MS; Figure 3b) indicate no measurable tectonic rotation with respect to the Australian plate during the Miocene (Figure 9a). A similar, small, tilt-corrected declination at locality MB just south of the Rakauroa Fault (Figure 3b) is also consistent with negligible tectonic rotation (Figure 9b), but in the absence of constraints from field tests, the possibility of a late remagnetization cannot be excluded in this case. The spatial distribution of these localities indicates that the boundary between the unrotated and rotated parts of the Hikurangi margin runs ENE, between the Rakauroa and Waerengaokuri faults, before intersecting the coast north of Tolaga Bay (Figure 10a). This ENE-WSW trend contrasts with previous studies, which have proposed a NW-SE trending boundary running between the Bay of Plenty and Gisborne, with differential rotation being accommodated by dextral strike slip on the Otoko-Totangi, Rakauroa and Waerengaokuri faults [e.g., Lamb, 1988].

[28] For the central Hikurangi margin (the “Wairoa” domain of Walcott [1989]), the best constrained data come from the coastal region, where declinations of  $50\text{--}60^\circ$  recorded by late Miocene–Pliocene remagnetizations at Mahia Peninsula (TC, PP and NR) and at localities TP and MP, and the  $90^\circ$  declination of the early forming remanence at WU, represent tectonic rotations with respect to the Australian plate of  $45\text{--}55^\circ$  and  $\sim 80^\circ$ , respectively. Such large rotations cannot be accounted for by long-term rotation of the Hikurangi margin at the presently observed rate of  $2.8\text{--}3.8^\circ \text{ Ma}^{-1}$  [Wallace *et al.*, 2004] (Figure 9a). Data from further inland are more difficult to interpret due

**Figure 9.** (a) Plots of corrected declinations versus magnetization age for localities where the timing of remanence acquisition can be constrained by field tests. Dotted lines indicate predicted declinations from extrapolation of tectonic rotation at present-day rates (hatched area) [Wallace *et al.*, 2004] and from higher rates before 1–2 Ma (these rates exclude the  $1^\circ \text{ Ma}^{-1}$  clockwise rotation due to drift of the Australian plate [Idnurm, 1985], which is also plotted). The shaded area represents a best fit rotation history based on these data. (b) Tilt-corrected declinations plotted against depositional age for localities where the timing of remanence acquisition could not be constrained by field tests. Data for some localities fall below the best fit rotation history from Figure 9a, suggesting that they have been remagnetized. (c) Previously published paleomagnetic data from the Hikurangi margin [Walcott *et al.*, 1981; Walcott and Mumme, 1982; Mumme and Walcott, 1985; Wright and Walcott, 1986; Lamb, 1988; Roberts, 1992; Vickery and Lamb, 1995], plotted against the best fit rotation history from Figure 9a. Smaller, light grey diamonds mark localities thought by Rowan *et al.* [2005] to be compromised by strong PDF overprints.

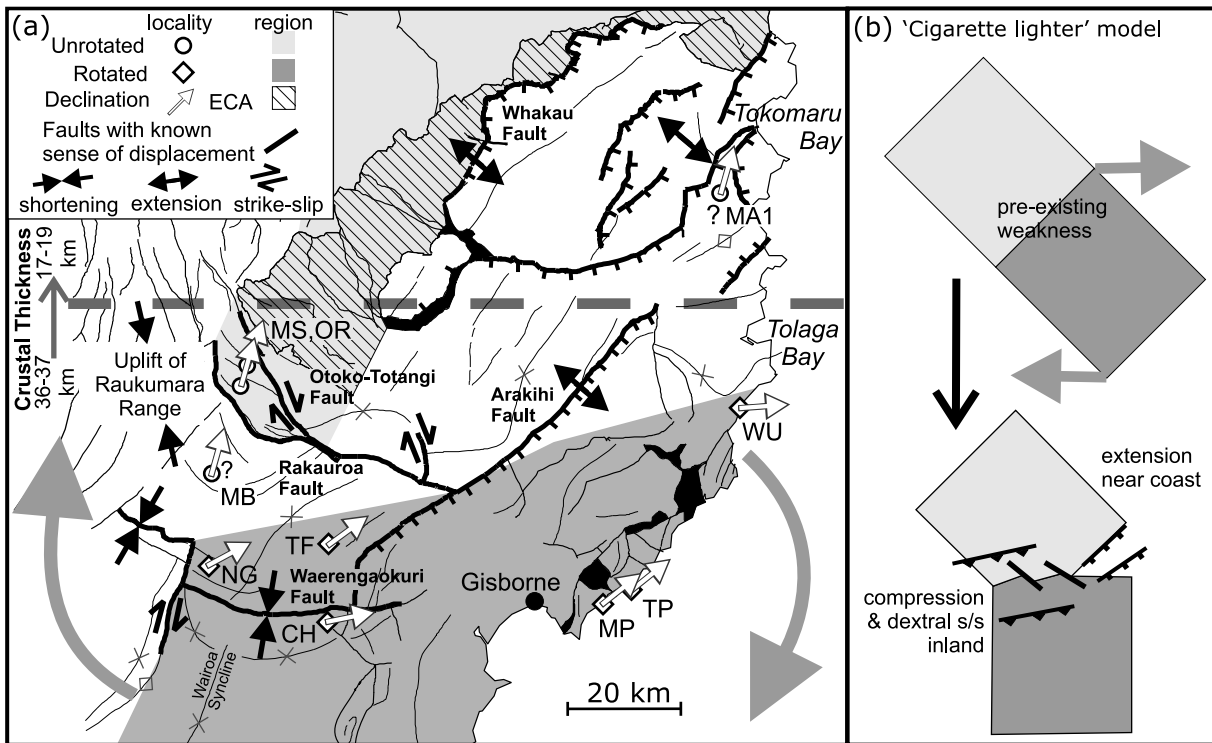


**Figure 10.** (a) Paleomagnetically defined limits of the rotating and nonrotating parts of the Hikurangi margin on Raukumara Peninsula. Localities with well-constrained magnetizations have been plotted with white arrows depicting their inferred clockwise rotations. The small declination anomaly at MB, and the unrotated, reversed polarity magnetization at locality MA1 reported by *Mumme et al.* [1989], are not used to constrain the rotation boundary because the ages of remanence acquisition are unconstrained. Inferred senses and directions of horizontal strain have been plotted for active faults (marked in bold). The thick dashed line marks the approximate location of an abrupt change in the thickness of the Australian plate. Early Miocene thrust sheets are defined by the East Coast Allochthon (ECA). (b) Schematic representation of a “cigarette lighter” model, in which differential rotations are being accommodated by a combination of extension near the coast, and compression and dextral strike-slip inland.

to large uncertainties in the timing of remanence acquisition; however, the declinations of  $50\text{--}60^\circ$  recorded at localities TF and NG appear to be carried by late forming magnetizations, which formed closer to Pliocene folding than to middle Miocene deposition (section 3.3.1). If this is the case, then assuming that the presently observed regional deformation pattern has persisted during the Quaternary (see section 1), a best fit for all of the new data from the central Hikurangi margin requires rotation rates of  $8\text{--}14^\circ \text{Ma}^{-1}$  relative to the Australian plate (most likely  $\sim 9^\circ \text{Ma}^{-1}$ ) between  $7\text{--}10 \text{ Ma}$  and  $1\text{--}2 \text{ Ma}$  (shaded region on Figure 9a). Further south along the Hikurangi margin, the declination of  $60 \pm 2^\circ$  for a late Miocene–Pliocene synfolding magnetization from southern Hawke Bay (localities WT, BH, and TI), an area previously considered to be part of the “Wairarapa” domain (Figure 1b), is also consistent with higher rates of tectonic rotation during the late Miocene and Pliocene (Figure 9a). The geographical spread of the data in Figure 9a is sufficient to indicate that rather than being divided into discrete regions with separate tectonic histories, a  $\sim 400 \text{ km}$  section of the Hikurangi margin between Tolaga Bay and Cook Strait appears to have been rotating coherently since the late Miocene.

[29] Although there are few reliable data in our reduced data set regarding middle and early Miocene rotation of the central and southern margin, there is some evidence of substantially reduced tectonic rotation rates before  $7\text{--}10 \text{ Ma}$ . On the southern Hikurangi margin, the apparently early Miocene magnetization at locality OK records only  $10\text{--}15^\circ$  of additional rotation relative to the Australian plate compared to the late Miocene–Pliocene magnetizations in southern Hawke Bay (Figure 9a), similar to that expected from large-scale motion of the Australian plate during this period, and consistent with no tectonic rotation before  $\sim 7 \text{ Ma}$ . On the central Hikurangi margin, similar declinations of  $80\text{--}90^\circ$  are recorded both by the early forming, late Miocene magnetization at locality WU and the middle Miocene sediments at locality CH. Although a late Miocene remagnetization at CH cannot be ruled out, the large tectonic rotations observed at these localities approach the maximum suggested by even the most radical tectonic reconstructions [e.g., *Rait et al.*, 1991]. The additional  $\sim 20^\circ$  of tectonic rotation observed north of Hawke Bay potentially indicates that rotation initiated  $1\text{--}2 \text{ Ma}$  earlier in this region than in the south, but the data are insufficient to definitively establish this. It is also possible that localities further inland (TF, NG, and CH) record a slightly lower late

**Table 3.** Known and Inferred Intraplate Deformation Involved in Accommodating Coherent Fore-Arc Rotation<sup>a</sup>

	Period, Ma		
	10–5	5–1.5	1.5–0
Required Deformation, <sup>b</sup> km	190	170	25
Known/estimated deformation by region, km			
TVZ/CVR (E) <sup>c</sup>	–	≤70	≤10
Raukumara Peninsula (T/E)	?	≤20 <sup>d</sup>	
Northern Taranaki Basin (E) <sup>e</sup>	≤5	–	–
Southern Taranaki Basin (T) <sup>f</sup>	≤100	–	–
Wairarapa (T) <sup>g</sup>	20	20	10
Marlborough Fault Zone (S/S)		≤105 <sup>h</sup>	~20 <sup>i</sup>
Total known/estimated deformation, km	≤125	≤210	≤140

<sup>a</sup>E is extension, T is thrusting/compression, and S/S is strike-slip.

<sup>b</sup>Required to accommodate the coherent rotations inferred from paleomagnetic data.

<sup>c</sup>Volcanic arc migration rate from *Cole et al.* [1995], modified according to rotation history in Figure 9.

<sup>d</sup>Total deformation since 5 Ma, estimated from Figure 10.

<sup>e</sup>*King and Thrasher* [1992].

<sup>f</sup>Maximum shortening estimated by *Stern et al.* [2006].

<sup>g</sup>Pliocene-Quaternary shortening from *Nicol and Beavan* [2003].

<sup>h</sup>Calculated from the rotation poles of *Cande and Stock* [2004] assuming 80% of interplate motion was accommodated on the MFZ.

<sup>i</sup>Calculated from *Cande and Stock* [2004] assuming that 50% of margin-parallel fore-arc motion is being expressed as internal deformation (on the NIDFB) rather than as rotation.

Miocene–Pliocene rate of rotation (but still  $\geq 5^\circ \text{ Ma}^{-1}$  with respect to the Australian plate) than is observed at coastal localities, but it is more likely that this is a reflection of the large uncertainties in the age of remanence acquisition at these localities, rather than a robust systematic difference.

#### 4.2. Implications of Widespread Remagnetizations

[30] Difficulties in obtaining good paleomagnetic data from New Zealand Cenozoic sediments, due to their weak magnetization and strong PDF overprints, have been well documented in previous studies [e.g., *Walcott and Mumme*, 1982; *Mumme et al.*, 1989; *Turner et al.*, 1989; *Pillans et al.*, 1994; *Roberts et al.*, 1994; *Turner*, 2001; *Rowan et al.*, 2005]. Our results reemphasize these problems; stable ChRMs without strong PDF overprints were routinely isolated at only 33% of the localities sampled. However, another potential difficulty with paleomagnetic data from the Hikurangi margin, that has not been appreciated in previous tectonic studies, is the presence of late forming magnetizations in these sediments, as a consequence of the widespread growth of authigenic greigite during late diagenesis [*Rowan and Roberts*, 2005, 2006]. Our results make the scale of this problem clear: at least 9, and possibly 12, of the 16 localities where the timing of remanence acquisition can be constrained have been remagnetized, often several million years after deposition. At localities where the timing of remanence acquisition could not be established, comparison of tilt-corrected declinations to the best fit rotation history provided by well-constrained data suggests that a further 3 localities (BP, NP, TH) may not record a depositional signal (Figure 9b). If this is the case, then at least 15 out of the 23 stably magnetized localities reported in this study (65%) carry late forming magnetizations, and the broad scatter of declinations seen in Figure 7 is explained by the fact that at many localities, the age of the magnetization does not correlate with the age of the sediments. Widespread remagnetization of sediments on the Hikurangi

margin also make it likely that data from previous studies, which were assumed to represent a depositional paleomagnetic signal but are not usually constrained by structural field tests, are similarly affected by late forming magnetizations (Figure 9c). Only declinations from the Marlborough region [*Roberts*, 1992, 1995a] (squares in Figure 9c), which correlate well with deviations in the strike of a vertical structural fabric in the Torlesse basement rocks [*Little and Roberts*, 1997], appear to be unaffected by late remagnetizations, and these data also indicate fast Pliocene rotation rates, comparable with those inferred for the North Island in this study.

#### 4.3. Comparison of Long-Term Rotation Patterns With Active Deformation

[31] Present-day rotation of the Australia-Pacific plate boundary in the New Zealand region is driven by a couple arising from the transition from subduction to intracontinental transpression (Figure 1a). Vertical axis rotations on the Australian plate therefore arise as a passive response to the reorientation of the subducting Pacific plate [*Walcott*, 1989]; the dominant role of large-scale boundary forces is reflected by the similar rates of rotation along the whole Hikurangi fore arc observed in the short-term velocity field [*Wallace et al.*, 2004] (Figure 1a). Although data from the southern North Island remain limited, the rigorously constrained paleomagnetic data presented here indicate similar rates and magnitudes of tectonic rotation along the whole Hikurangi margin south of Tolaga Bay since the late Miocene, which strongly suggests that they are a result of the same forces, acting over geological timescales. Coherent rotation of a large section of the East Coast region therefore appears to be a feature of both long- and short-term deformation on the Hikurangi margin. However, there are features of the long-term deformation pattern that still conflict with the short-term velocity field. These features include the negligible Neogene tectonic rotations on the northern Raukumara Peninsula (section 4.1), which presently appears to be rotating at the same rate as the rest of the Hikurangi margin [*Wallace et al.*, 2004; *Nicol and Wallace*, 2007] (Figure 1a), and the more rapid late Miocene–Pliocene rotation of the central and southern Hikurangi margin, at rates at least twice those presently observed. If real, these apparent changes in the extent and movement of the rotating block must reflect temporal changes in how tectonic rotation of the Hikurangi margin has been structurally accommodated within the fore arc.

#### 4.4. Structural Accommodation of Large Rotations

[32] Despite the significant spatial variations in vertical axis rotations along the Hikurangi margin proposed in previous studies, many authors have presumed that vertical axis rotations have been a feature of the developing subduction zone since the early Miocene [e.g., *Wright and Walcott*, 1986]. In contrast, our data suggest little significant rotational deformation during the early and middle Miocene, with initiation of widespread tectonic rotation south of the Raukumara Peninsula only occurring at 8–10 Ma. Another significant change occurred at ~5 Ma, when tectonic rotations initiated in northeast Marlborough; we also suggest that the establishment of the present tectonic regime at 1.5–2 Ma slowed margin rotation to rates

comparable with those inferred from geodetic studies. These studies also suggest a possible northward expansion of the rotating region to include the Raukumara Peninsula. These inferred transitions possibly mark significant changes in the structures and mechanisms involved in accommodating vertical axis rotations on the Hikurangi margin, even if, as discussed in section 4.3, the underlying geodynamic forces driving these rotations have remained constant.

[33] Coherent rotation of the Hikurangi margin does not necessarily imply that the fore arc is acting as a single rigid “microplate”; the short-term velocity field indicates negligible differential rotations within the Hikurangi fore arc despite significant internal deformation, principally associated with basement faults of the NIDFB (Figure 1a) [Wallace *et al.*, 2004]. As a consequence, however, most rotational deformation must ultimately be accommodated by structures at the edges of the deforming region, as demonstrated by the key roles of the TVZ and Marlborough Fault Zone (MFZ) in the present tectonic regime. The large and coherent rotations indicated by our paleomagnetic data require that analogous structures must have been active throughout the last 10 Ma and that they must have accommodated a significant amount of deformation: even with a local pole of rotation, a 70–80° rotation of a 300–400 km section of fore arc requires ~400 km of cumulative deformation at its edges. Although the distribution and density of reliable paleomagnetic data are still insufficient to fully delineate the extent of the deforming plate boundary zone, our revised rotation history allows tectonic rotations on the Hikurangi margin to be more plausibly related to known structures, which, as we discuss in the following sections, can account for a significant fraction of the required intraplate deformation (Table 3).

#### 4.4.1. Northern Limit of Rotation

[34] On the Raukumara Peninsula, paleomagnetic data indicate that the northern limit of Neogene tectonic rotation is confined to a 10-km-wide zone between the Rakauroa and Waerengaokuri faults inland, and to a 25 km stretch between Tolaga Bay and Tokomaru Bay on the coast (Figure 10a). The ENE-WSW trending boundary region coincides with an abrupt reduction in crustal thickness on the Australian plate north of Tolaga Bay [Davey *et al.*, 1997; Reyners *et al.*, 1999] (Figure 2), which has reduced the downdip extent of the seismogenic zone [Reyners, 1998; Reyners and McGinty, 1999]. This, combined with the presence of sediments with high pore fluid pressure at the plate interface [Collot *et al.*, 1996; Reyners *et al.*, 1999], produces a sharp decrease in interplate coupling between Gisborne and Tolaga Bay [Reyners, 1998], which might play an important role in allowing large differential rotations between the northern Raukumara Peninsula and the rest of the Hikurangi margin.

[35] Establishing the sense, magnitude and timing of movement on the numerous Neogene faults in the northern hinge area is complicated by uplift and erosion of the sedimentary cover, but a clear change in tectonic style can be identified across the boundary zone. In the northeast, most faults with large (>100 m) displacements are north to northeast trending normal faults [Thornley, 1996] (Figure 10a). To the south, NE-SW trending structures such as the Wairoa Syncline begin to dominate [Mazengarb and Speden, 2000], indicating margin-perpendicular shortening.

Inland of the area between Tolaga Bay and Gisborne, however, structures consistent with approximately N-S shortening (e.g., the Waerengaokuri Fault, and the southward plunge of the Wairoa Syncline) and dextral strike slip (e.g., the Otoko-Totangi Fault) are superimposed on this general pattern (Figure 10a). A combination of extension toward the coast and shortening inland, which may also have contributed to uplift of the Raukumara Range, therefore appear to have accommodated differential rotations in this region, hinged about a zone near the intersection of the Waerengaokuri and Arakihi faults. This mechanism mimics the opening of a cigarette lighter, as schematically illustrated in Figure 10b.

[36] Visual inspection of Figure 10a suggests that ~45° of differential rotation has been accommodated in the region delineated by paleomagnetic data, which is at most 70% of the 60–80° of rotation indicated by the oldest declination anomalies in this region (CH, WU). Contemporary rotation of the Raukumara Peninsula inferred from the short-term velocity field has been cited as evidence that the Raukumara rotation boundary has been inactive during the Quaternary [Nicol and Wallace, 2007] and that more recent rotational deformation has been accommodated on unidentified structures further to the north. Conversely, the clear change in interplate coupling observed in this region and the late Quaternary scarps on several of the faults highlighted in Figure 10a [Thornley, 1996] suggest that the hinge could still be active and that the presently observed structures, most of which are Pliocene or younger in age [Field *et al.*, 1997], may have obscured an earlier period of deformation (i.e., they have accommodated only the last 5–6 Ma of differential rotation). The paucity of late Miocene or younger paleomagnetic data north of the rotation boundary currently makes it difficult to test either hypothesis.

[37] Regardless of its timing, deformation associated with the rotation boundary in Figure 10a is unlikely to account for more than a few km of the deformation required to accommodate coherent fore-arc rotation (Table 3). A more significant contribution comes from back-arc extension in the TVZ since 2 Ma [Wilson *et al.*, 1995], and in the wider Central Volcanic Region (CVR) from ~5 Ma [Stern, 1987], when back-arc rifting began in the Havre Trough to the north of New Zealand [Wright, 1993]. A 30° clockwise rotation of the Hikurangi volcanic arc in the last 4 Ma [Stern *et al.*, 2006], which is entirely consistent with our paleomagnetically determined fore-arc rotation history (Figure 9), suggests that the western boundary of rotation is associated with this rifting. The average arc migration rate of  $21 \pm 3 \text{ mm a}^{-1}$  [Cole *et al.*, 1995] (compared to 5–15  $\text{mm a}^{-1}$  of contemporary extension in the TVZ reported by Wallace *et al.* [2004]) provides a maximum estimate of ~80 km of Pliocene-Quaternary back-arc extension. In contrast, other than limited late Miocene extension in the northern Taranaki Basin [King and Thrasher, 1992], any evidence of earlier deformation west of the Raukumara Range has been obscured by younger volcanism and tectonism in the CVR/TVZ.

#### 4.4.2. Southern Limit of Rotation

[38] Paleomagnetic studies have established that there were no tectonic rotations in the Marlborough region during the middle-late Miocene [Roberts, 1992]. At this time, it is likely that the southern limit of rotation was associated with Cook Strait, which appears to represent a major structural

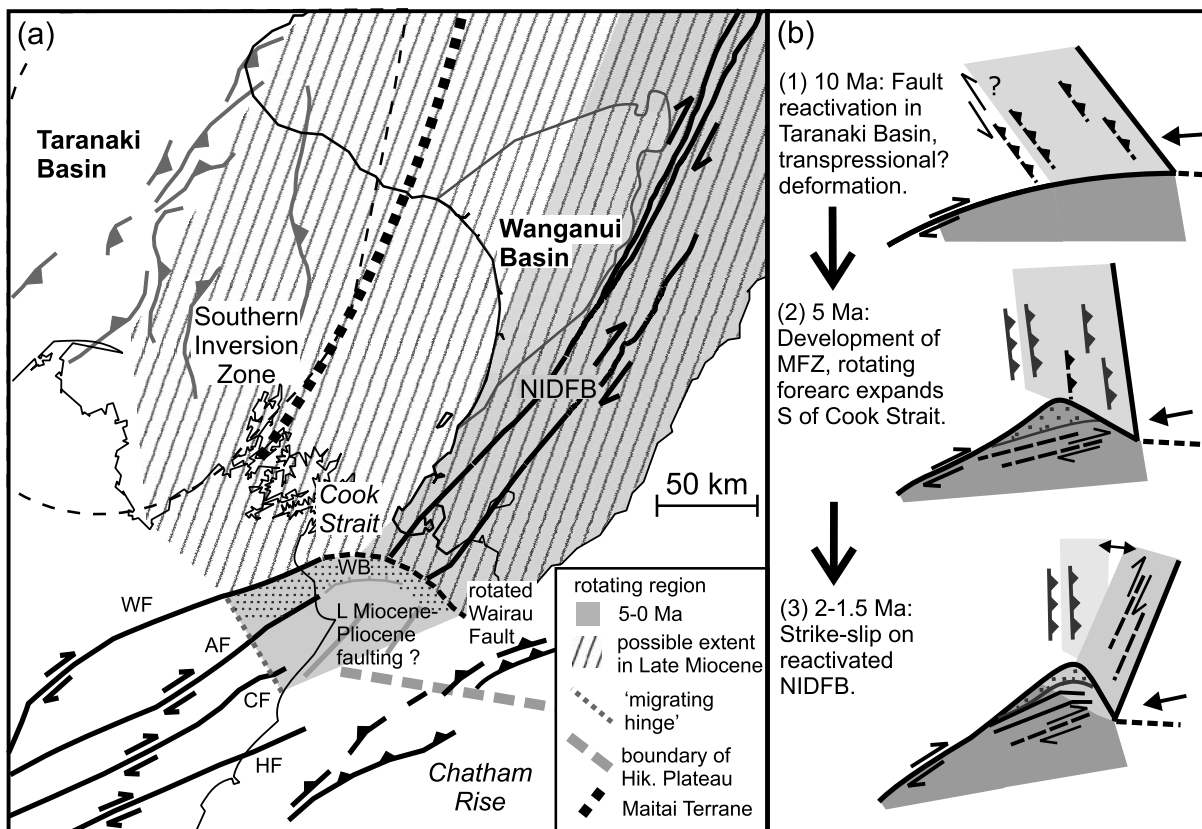


**Figure 11.** (a) Deformation patterns in the southern North Island and northeastern South Island of New Zealand, including major strike-slip faults (NIDFB, North Island Dextral Fault Belt; WF, Wairau Fault; AF, Awatere Fault; CF, Clarence Fault; HF, Hope Fault), late Miocene thrusts in the Taranaki Basin (Southern Inversion Zone), and the probable distribution of Neogene tectonic rotations, the southern boundary of which is associated with the boundary between the Hikurangi Plateau and continental crust of Chatham Rise. The inactive eastern termination of the Wairau Fault curves through Cook Strait. WB, Wairau Basin. Partially adapted from *Barnes and Audru* [1999] according to *Little and Roberts* [1997]. (b) Proposed model of Neogene deformation in this region (see section 4.4.2).

discontinuity [Walcott, 1978] (Figure 11a). The faults of the NIDFB cannot be directly linked across Cook Strait to those in the MFZ [Carter *et al.*, 1988], and Mesozoic basement terranes are offset by 140 km across what is interpreted to be the eastern termination of the Wairau Fault, which is bent up to 90° clockwise through Cook Strait [Walcott, 1978; Lewis *et al.*, 1994]. This feature alone suggests that significant rotational deformation has been accommodated in this region during the Neogene. The southern limit of rotation also appears to be fundamentally linked to an abrupt increase in crustal thickness on the Pacific plate in this region, which marks the boundary between the Hikurangi Plateau and continental crust of Chatham Rise [Eberhart-Phillips and Reyners, 1997; Reyners, 1998] (Figure 2). Increased interplate coupling across this transition appears to have permanently locked the plate interface off the coast of Marlborough [Collot *et al.*, 1996; Barnes and Mercier de Lepinay, 1997], with the result that >80% of relative plate motion is currently being accommodated by the MFZ [Holt and Haines, 1995]; the “migrating hinge” which marks the southern limit of Pliocene-Quaternary rotations in northern Marlborough is also associated with this boundary [Little and Roberts, 1997] (Figure 11a).

[39] The apparent initiation of widespread vertical axis rotation at 8–10 Ma coincided with a period of tectonic activity over a large area of the southern North Island [King, 2000; Nicol *et al.*, 2002]. The western limit of this activity was in the Taranaki Basin, where Cretaceous normal faults in the southern basin were reactivated as reverse faults (the Southern Inversion Zone of King and Thrasher [1992]; Figure 11a). Like the TVZ and NIDFB, the North Island axial ranges (Figure 2), which currently act as a backstop to the deforming Hikurangi margin [Nicol and Beavan, 2003], are geologically young [e.g., Beu *et al.*, 1981; Erdman and Kelsey, 1992; Nicol *et al.*, 2002]; it is therefore possible that during the late Miocene the plate boundary region extended much further west and that the shortening in the Southern Inversion Zone accommodated rotation of a much wider fore arc (Figure 11). Our proposed rotation history predicts ~30° of late Miocene rotation (Figure 9), which could potentially explain the long-wavelength curvature of Mesozoic basement terranes through the western North Island, including the Maitai Terrane/Junction Magnetic Anomaly [Sutherland, 1999b] (Figures 1a and 11a), the origin and timing of which remains controversial [e.g., Bradshaw *et al.*, 1996; Sutherland, 1999a]. Although small to moderate

( $-10$  to  $40^\circ$ ) declinations have been reported from Oligocene–early Miocene sediments in this region [Mumme and Walcott, 1985], the use of blanket demagnetization techniques, and the lack of any constraint on the timing of remanence acquisition, make it difficult to assess the significance of these data.

[40] In the Southern Inversion Zone, up to 3 km of exhumation is indicated by offset porosity-depth trends [Armstrong *et al.*, 1998] and thermal modeling [Funnell *et al.*, 1996]; lower crustal thickening observed in deep seismic reflection profiles indicates total Neogene shortening of  $70 \pm 30$  km [Stern *et al.*, 2006], although this is not necessarily confined to the late Miocene. There was also a moderate amount of late Miocene shortening on reverse faults in the Wairarapa region, including the faults that presently comprise the NIDFB (Table 3). If faulting in the western South Island marked the edge of the tectonically rotating region in the late Miocene, interplate deformation would have been focused away from the eastern Wairau Fault, causing it to rotate with the rest of the Hikurangi margin to the north (Figure 11b). The deformation recorded by late Miocene–Pliocene faulting across Cook Strait is poorly constrained [Barnes and Audru, 1999], but extension in the late Miocene Wairau Basin [Lewis *et al.*, 1994] was probably involved in accommodating this rotation, which eventually led to formation of the MFZ at  $\sim 5$  Ma, to allow the more efficient transfer of interplate motion onto the Alpine Fault. Since that time, the southern boundary of the rotating fore arc has been the migrating hinge of Little and Roberts [1997], meaning that southwestward translation and rotation of the southern Hikurangi fore arc has been ultimately accommodated by the MFZ (Figure 11b).

[41] In the present tectonic regime, 35–75% of the dextral strike-slip that is partitioned into the Hikurangi fore arc is associated with internal deformation on the NIDFB [Wallace *et al.*, 2004], rather than tectonic rotation. Quaternary reactivation of these faults as dextral strike-slip faults [Beanland, 1995; Beanland *et al.*, 1998] resulted from clockwise rotation of the Hikurangi margin relative to a stable Aus-Pac convergence vector [Cande and Stock, 2004], which led to increased obliquity and partitioning of margin-parallel strain into the fore arc. It is therefore possible that during the Pliocene, when the NIDFB was not active, that all MFZ slip (up to 105 km, assuming 80% of 130 km total interplate motion [Cande and Stock, 2004]) was accommodating rotational deformation of the Hikurangi margin. Relatively strong interplate coupling at the subduction interface has also resulted in the transfer of  $\sim 30$  km of margin-perpendicular shortening into the southern Hikurangi fore arc since 5 Ma, primarily on faults east of the Mohaka Fault [Nicol and Beavan, 2003]. This shortening contrasts with weaker interplate coupling and Pliocene–Quaternary extension in the north (section 4.4.1), and hence is also associated with rotational deformation.

#### 4.4.3. Summary

[42] As summarized in Table 3, known deformation within the New Zealand plate boundary region, predominantly in the CVR/TVZ and MFZ, appears to be sufficient to account for large-scale, coherent rotation of the Hikurangi margin in the past 5 Ma, even with the much higher rates of tectonic rotation during the Pliocene implied by our paleomagnetic data. In the late Miocene, however, only 125

km out of 190 km ( $\sim 65\%$ ) of the required deformation can potentially be accounted for, and the principal component of this estimated deformation (the crustal thickening beneath the Taranaki Basin) has uncertain timing. Deformation in the northern fore arc from 10 to 5 Ma is also poorly characterized, however, and the large and rapid rotations of the margin implied by our paleomagnetic data also raise the possibility of late Miocene oblique convergence, and associated strain partitioning. These uncertainties could be greatly reduced by further paleomagnetic sampling west of the present Hikurangi margin, to test the link between deformation in the western North Island and late Miocene fore-arc rotation.

#### 4.5. Rotation, Remagnetization, and Collision of the Hikurangi Plateau

[43] Limited paleomagnetic data for the early and middle Miocene indicate no widespread tectonic rotations on the North Island in this time period, despite subduction of the Pacific plate since 23–20 Ma [Rait *et al.*, 1991; King, 2000]. As discussed above, active rotation of the margin appears to be linked to subduction of the Hikurangi Plateau, the downdip extent of which is still poorly resolved. Thickened oceanic crust has been inferred on the subducted slab at depths of 15 to 30 km using ScSp conversions [Bourne and Stuart, 2000], and down to depths of 65 km by recent tomographic studies [Reyners *et al.*, 2006]. This represents  $\sim 7$  Ma of subduction, and suggests that initiation of vertical axis rotations on the Hikurangi margin may be linked to collision of the Hikurangi Plateau with the subduction margin in the early late Miocene, a period of shortening and tectonic uplift along the entire Hikurangi margin [Buret *et al.*, 1997; King, 2000; Nicol *et al.*, 2002]. This regional tectonic episode also appears to be linked to widespread remagnetization of sediments along the Hikurangi margin: at well constrained sites (Figure 9a), remanence acquisition dates cluster at 5–8 Ma, and similar timings are indicated for unconstrained sites if tectonic rotations are extrapolated onto the best fit rotation pattern (Figures 9b and 9c). Anomalous magnetizations carried by iron sulfides have been linked to migration of gas hydrates [Housen and Musgrave, 1996; Larrasoana *et al.*, 2007], or to hydrocarbon seepage [Reynolds *et al.*, 1994], both of which are potential consequences of the deformation resulting from collision of the Hikurangi Plateau.

### 5. Conclusions

[44] New paleomagnetic results from New Zealand, when properly constrained by field tests, provide important new insights into Neogene tectonic rotations on the Hikurangi margin. Our data indicate that large-scale plate boundary forces drive coherent, long-term rotational deformation of the margin, in agreement with the short-term velocity field. Previously reported lateral variations in the rate and magnitude of tectonic rotations south of the Raukumara Peninsula are probably an effect of unrecognized late remagnetizations involving the iron sulfide greigite, which have affected up to 65% of the stably magnetized localities reported here. The mechanism causing the widespread growth of iron sulfides several million years after deposition is poorly understood, but may be linked to uplift and

methane hydrate dissociation caused by a regional tectonic event on the Hikurangi margin, possibly associated with collision of the Hikurangi Plateau, in the late Miocene.

[45] To account for clockwise rotations of up to  $80^\circ$  since 7–10 Ma,  $50\text{--}60^\circ$  of which occurred since 5–6 Ma, rotation rates of  $8\text{--}14^\circ \text{Ma}^{-1}$  with respect to the Australian plate, which are much higher than the present rate of  $3\text{--}4^\circ \text{Ma}^{-1}$ , are required before 1–2 Ma. Difficulties in obtaining reliable paleomagnetic data, due to widespread late remagnetizations and strong present-day field overprints, mean that rotation of the Hikurangi margin before the late Miocene remains relatively unconstrained, but present data suggest that rates of tectonic rotation were substantially reduced, and possibly zero, before 8–10 Ma. The northern and southern limits of the rotating fore arc appear to have remained relatively fixed, and are associated with major lateral changes in basement structure of the Hikurangi margin that have maintained long-term discontinuities in intraplate coupling. In contrast, the late Miocene plate boundary zone may have extended much further into the western North Island, and structures in this region may have played an important role in accommodating the large rotations indicated by the paleomagnetic data.

[46] **Acknowledgments.** This research was supported by the U.K. Natural Environment Research Council (grant NER/S/2001/06363). Figure 2 was generated using the QMAP data set, provided by the Institute of Geological and Nuclear Sciences (IGNS). We thank Colin Mazengarb and Julie Lee from IGNS, Gillian Turner and Tim Little from Victoria University of Wellington, and Geoff Rait for valuable information and logistical support during fieldwork and Andy Nicol, Rupert Sutherland, Laura Wallace, and an anonymous reviewer for comprehensive comments on an earlier version of this paper.

## References

- Ansell, J. H., and S. C. Bannister (1996), Shallow morphology of the subducted Pacific plate along the Hikurangi margin, New Zealand, *Phys. Earth Planet. Inter.*, *93*, 3–20.
- Armstrong, P. A., R. G. Allis, R. H. Funnell, and D. S. Chapman (1998), Late Neogene exhumation patterns in Taranaki Basin (New Zealand): Evidence from offset porosity-depth trends, *J. Geophys. Res.*, *103*, 30,269–30,282.
- Barnes, P. M., and J. C. Audru (1999), Quaternary faulting in the offshore Flaxbourne and Wairarapa basins, southern Cook Strait, New Zealand, *N. Z. J. Geol. Geophys.*, *42*, 349–367.
- Barnes, P. M., and B. M. Mercier de Lepinay (1997), Rates and mechanics of rapid frontal accretion along the very obliquely convergent southern Hikurangi margin, New Zealand, *J. Geophys. Res.*, *102*, 24,931–24,952.
- Beanland, S. (1995), The North Island dextral fault belt, Hikurangi subduction margin, New Zealand, Ph.D. thesis, Victoria Univ. of Wellington, New Zealand.
- Beanland, S., A. Melhuish, A. Nicol, and J. Ravens (1998), Structure and deformational history of the inner forearc region, Hikurangi subduction margin, New Zealand, *N. Z. J. Geol. Geophys.*, *41*, 325–342.
- Beu, A. G., G. H. Browne, and T. L. Grant-Taylor (1981), New *Chlamys-Delicatula* localities in the central North Island and uplift of the Ruahine Range, *N. Z. J. Geol. Geophys.*, *24*, 127–132.
- Bourne, M., and G. Stuart (2000), ScSp observed on North Island, New Zealand: Implications for subducting plate structure, *Geophys. J. Int.*, *142*, 925–932.
- Bradshaw, J. D., S. D. Weaver, and R. J. Muir (1996), Mid-Cretaceous oroclinal bending of New Zealand terranes, *N. Z. J. Geol. Geophys.*, *39*, 461–468.
- Buret, C., F. Chanier, J. F erri ere, and J. N. Proust (1997), Individualization of a forearc basin during the active margin evolution: Hikurangi subduction margin, New Zealand, *C. R. Acad. Sci., Ser. IIA*, *325*, 615–621.
- Cande, S. C., and J. M. Stock (2004), Pacific-Antarctic-Australia motion and the formation of the Macquarie plate, *Geophys. J. Int.*, *157*, 399–414, doi:10.1111/j.1365-246X.2004.02224.x.
- Carter, L., K. B. Lewis, and F. Davey (1988), Faults in Cook Strait and their bearing on the structure of central New Zealand, *N. Z. J. Geol. Geophys.*, *31*, 431–446.
- Chanier, F., and J. F erri ere (1989), On the existence of major tangential movements in the East Coast Range of New Zealand—Their significance within the framework of Pacific plate subduction, *C. R. Acad. Sci., Ser. II*, *308*, 1645–1650.
- Cole, J. W., D. Darby, and T. Stern (1995), Taupo Volcanic Zone and Central Volcanic Region: Backarc structures of North Island, New Zealand, in *Backarc Basins*, edited by B. Taylor, pp. 1–28, Springer, New York.
- Collot, J. Y., et al. (1996), From oblique subduction to intra-continental transpression: Structures of the southern Kermadec–Hikurangi margin from multibeam bathymetry, side-scan sonar and seismic reflection, *Mar. Geophys. Res.*, *18*, 357–381.
- Davey, F. J., S. Henrys, and E. Lodolo (1997), A seismic crustal section across the East Cape convergent margin, New Zealand, *Tectonophysics*, *269*, 199–215.
- Davies, E. J., J. B. Frederick, W. L. Leask, and T. J. Williams (2000), East Coast drilling results, paper presented at New Zealand Petroleum Conference, Crown Miner. Group, Auckland, New Zealand, 19–22 March.
- Davy, B., and R. Wood (1994), Gravity and magnetic modelling of the Hikurangi Plateau, *Mar. Geol.*, *118*, 139–151.
- Demarest, H. H. (1983), Error analysis for the determination of tectonic rotation from paleomagnetic data, *J. Geophys. Res.*, *88*, 4321–4328.
- Eberhart-Phillips, D., and M. Reyners (1997), Continental subduction and three-dimensional crustal structure: The northern South Island, New Zealand, *J. Geophys. Res.*, *102*, 11,843–11,861.
- Erdman, C. F., and H. M. Kelsey (1992), Pliocene and Pleistocene stratigraphy and tectonics, Ohara Depression and Wakarara Range, North Island, New Zealand, *N. Z. J. Geol. Geophys.*, *35*, 177–192.
- Field, B. D., et al. (1997), *Cretaceous-Cenozoic Geology and Petroleum Systems of the East Coast Region*, *Inst. Geol. Nucl. Sci. Monogr.*, vol. 19, Ins. of Geol. and Nucl. Sci. Ltd., Lower Hutt, New Zealand.
- Fisher, R. A. (1953), Dispersion on a sphere, *Proc. R. Soc. London, Ser. A*, *217*, 295–305.
- Florindo, F., and L. Sagnotti (1995), Palaeomagnetism and rock magnetism in the upper Pliocene Valle Ricca (Rome, Italy) section, *Geophys. J. Int.*, *123*, 340–354.
- Francis, D., D. Bennett, and S. Courteney (2004), Advances in understanding of onshore East Coast Basin structure, stratigraphic thickness and hydrocarbon generation, paper presented at New Zealand Petroleum Conference, Crown Miner. Group, Auckland, New Zealand.
- Funnell, R., D. Chapman, R. Allis, and P. Armstrong (1996), Thermal state of the Taranaki Basin, New Zealand, *J. Geophys. Res.*, *101*, 25,197–25,215.
- Hall, L. S., S. H. Lamb, and C. MacNiocail (2004), Cenozoic distributed rotational deformation, South Island, New Zealand, *Tectonics*, *23*, TC2002, doi:10.1029/2002TC001421.
- Herzer, R. H. (1995), Seismic stratigraphy of a buried volcanic arc, Northland, New Zealand and implications for Neogene subduction, *Mar. Pet. Geol.*, *12*, 511–531.
- Holt, W. E., and A. J. Haines (1995), The kinematics of northern South Island, New Zealand, determined from geologic strain rates, *J. Geophys. Res.*, *100*, 17,991–18,010.
- Hong, C. S., M. Torii, K. S. Shea, and S. J. Kao (1998), Inconsistent magnetic polarities between greigite- and pyrrhotite/magnetite-bearing marine sediments from the Tsailiao-chi section, southwestern Taiwan, *Earth Planet. Sci. Lett.*, *164*, 467–481.
- Housen, B. A., and R. J. Musgrave (1996), Rock-magnetic signature of gas hydrates in accretionary prism sediments, *Earth Planet. Sci. Lett.*, *139*, 509–519.
- Idnurm, M. (1985), Late Mesozoic and Cenozoic palaeomagnetism of Australia. 1. A redetermined apparent polar wander path, *Geophys. J. R. Astron. Soc.*, *83*, 399–418.
- Jiang, W. T., C. S. Hong, A. P. Roberts, and D. R. Peacor (2001), Contradictory magnetic polarities in sediments and variable timing of neof ormation of authigenic greigite, *Earth Planet. Sci. Lett.*, *193*, 1–12.
- Kelsey, H. M., S. M. Cashman, S. Beanland, and K. Berryman (1995), Structural evolution along the inner forearc of the obliquely convergent Hikurangi margin, New Zealand, *Tectonics*, *14*, 1–18.
- King, P. R. (2000), Tectonic reconstructions of New Zealand: 40 Ma to the present, *N. Z. J. Geol. Geophys.*, *43*, 611–638.
- King, P. R., and G. P. Thrasher (1992), Post-Eocene development of the Taranaki Basin, New Zealand: Convergent overprint of a passive margin, in *Geology and Geophysics of Continental Margins*, edited by J. S. Watkin, F. Zhiqiang, and K. J. McMillen, *AAPG Mem.*, *53*, 93–118.
- Kingma, J. T. (1962), Geological map of New Zealand, sheet 11 Dannevirke, scale 1:250,000, Dep. of Sci. and Ind. Res., Wellington, New Zealand.
- Kirschvink, J. L. (1980), The least squares line and plane and the analysis of palaeomagnetic data, *Geophys. J. R. Astron. Soc.*, *62*, 699–710.

- Lamb, S. H. (1988), Tectonic rotations about vertical axes during the last 4 Ma in part of the New Zealand plate boundary zone, *J. Struct. Geol.*, *10*, 875–893.
- Larrasoana, J. C., A. P. Roberts, R. J. Musgrave, E. Gràcia, E. Piñero, M. Vega, and F. Martínez-Ruiz (2007), Diagenetic formation of greigite and pyrrhotite in gas hydrate marine sedimentary systems, *Earth Planet. Sci. Lett.*, *261*(3–4), 350–366, doi:10.1016/j.epsl.2007.06.032.
- Lee, J. M., and J. G. Begg (2002), Geology of the Wairarapa area, *Geol. Map 11*, scale 1:250,000, Inst. of Geol. and Nucl. Sci. Ltd., Lower Hutt, New Zealand.
- Lewis, K. B., L. Carter, and F. J. Davey (1994), The opening of Cook Strait—Interglacial tidal scour and aligning basins at a subduction to transform plate edge, *Mar. Geol.*, *116*, 293–312.
- Little, T. A., and A. P. Roberts (1997), Distribution and mechanism of Neogene to present-day vertical axis rotations, Pacific-Australian plate boundary zone, South Island, New Zealand, *J. Geophys. Res.*, *102*, 20,447–20,468.
- Mazengarb, C., and I. G. Speden (2000), Geology of the Raukumara area, *Geol. Map 6*, scale 1:250,000, Inst. of Geol. and Nucl. Sci. Ltd., Lower Hutt, New Zealand.
- McFadden, P. L., and M. W. McElhinny (1988), The combined analysis of remagnetisation circles and direct observations in palaeomagnetism, *Earth Planet. Sci. Lett.*, *87*, 161–172.
- Mumme, T. C., and R. I. Walcott (1985), Paleomagnetic studies at Geophysics Division 1980–1983, *Rep. 204*, Geophys. Div. Res., Dep. of Sci. and Ind. Res., Wellington.
- Mumme, T. C., S. Lamb, and R. I. Walcott (1989), The Raukumara paleomagnetic domain: Constraints on the tectonic rotation of the East Coast, N Island, New Zealand, from paleomagnetic data, *N. Z. J. Geol. Geophys.*, *32*, 317–326.
- Neef, G. (1992), The Cenozoic geology of the Gisborne area (1:50,000 metric sheet Y18AB), North Island, New Zealand, *N. Z. J. Geol. Geophys.*, *35*, 515–531.
- Nicol, A., and J. Beavan (2003), Shortening of an overriding plate and its implications for slip on a subduction thrust, central Hikurangi margin, New Zealand, *Tectonics*, *22*(6), 1070, doi:10.1029/2003TC001521.
- Nicol, A., and L. Wallace (2007), Temporal stability of deformation rates: Comparison of geological and geodetic observations, Hikurangi subduction margin, New Zealand, *Earth Planet. Sci. Lett.*, *258*, 397–413, doi:10.1016/j.epsl.2007.03.039.
- Nicol, A., R. Van Dissen, P. Vella, B. Alloway, and A. Melhuish (2002), Growth of contractional structures during the last 10 m.y. at the southern end of the emergent Hikurangi forearc basin, New Zealand, *N. Z. J. Geol. Geophys.*, *45*, 365–385.
- Pillans, B. J., A. P. Roberts, G. S. Wilson, S. T. Abbott, and B. V. Alloway (1994), Magnetostratigraphic, lithostratigraphic and tephrostratigraphic constraints on lower and middle Pleistocene sea-level changes, Wanganui Basin, New Zealand, *Earth Planet. Sci. Lett.*, *121*, 81–98.
- Rait, G. J. (2000), Thrust transport directions in the Northland Allochthon, New Zealand, *N. Z. J. Geol. Geophys.*, *43*, 271–288.
- Rait, G. J., F. Chanier, and D. W. Waters (1991), Landward- and seaward-directed thrusting accompanying the onset of subduction beneath New Zealand, *Geology*, *19*, 230–233.
- Reyners, M. (1983), Lateral segmentation of the subducted plate at the Hikurangi margin, New Zealand: Seismological evidence, *Tectonophysics*, *96*, 203–223.
- Reyners, M. (1998), Plate coupling and the hazard of large subduction thrust earthquakes at the Hikurangi subduction zone, New Zealand, *N. Z. J. Geol. Geophys.*, *41*, 343–354.
- Reyners, M., and P. McGinty (1999), Shallow subduction tectonics in the Raukumara Peninsula, New Zealand, as illuminated by earthquake focal mechanisms, *J. Geophys. Res.*, *104*, 3025–3034.
- Reyners, M., D. Eberhart-Phillips, and G. Stuart (1999), A three-dimensional image of shallow subduction: Crustal structure of the Raukumara Peninsula, New Zealand, *Geophys. J. Int.*, *137*, 873–890.
- Reyners, M., D. Eberhart-Phillips, G. Stuart, and Y. Nishimura (2006), Imaging subduction from the trench to 300 km depth beneath the central North Island, New Zealand, with Vp and Vp/Vs, *Geophys. J. Int.*, *165*, 565–583, doi:10.1111/j.1365-246X.2006.02897.x.
- Reynolds, R. L., M. L. Tuttle, C. A. Rice, N. S. Fishman, J. A. Karachewski, and D. M. Sherman (1994), Magnetization and geochemistry of greigite-bearing Cretaceous strata, North Slope Basin, Alaska, *Am. J. Sci.*, *294*, 485–528.
- Roberts, A. P. (1992), Paleomagnetic constraints on the tectonic rotation of the southern Hikurangi margin, New Zealand, *N. Z. J. Geol. Geophys.*, *35*, 311–323.
- Roberts, A. P. (1995a), Tectonic rotation about the termination of a major strike-slip fault, Marlborough Fault System, New Zealand, *Geophys. Res. Lett.*, *22*, 187–190.
- Roberts, A. P. (1995b), Magnetic properties of sedimentary greigite ( $\text{Fe}_3\text{S}_4$ ), *Earth Planet. Sci. Lett.*, *134*, 227–236.
- Roberts, A. P., and G. M. Turner (1993), Diagenetic formation of ferrimagnetic iron sulphide minerals in rapidly deposited marine sediments, South Island, New Zealand, *Earth Planet. Sci. Lett.*, *115*, 257–273.
- Roberts, A. P., and R. Weaver (2005), Multiple mechanisms of remagnetization involving sedimentary greigite ( $\text{Fe}_3\text{S}_4$ ), *Earth Planet. Sci. Lett.*, *231*, 263–277, doi:10.1016/j.epsl.2004.11.024.
- Roberts, A. P., G. M. Turner, and P. P. Vella (1994), Magnetostratigraphic chronology of late Miocene to early Pliocene biostratigraphic and oceanographic events in New Zealand, *Geol. Soc. Am. Bull.*, *106*, 665–683.
- Rowan, C. J., and A. P. Roberts (2005), Tectonic and geochronological implications of variably timed magnetizations carried by authigenic greigite in marine sediments from New Zealand, *Geology*, *33*, 553–556, doi:10.1130/G21382.1.
- Rowan, C. J., and A. P. Roberts (2006), Magnetite dissolution, diachronous greigite formation, and secondary magnetizations from pyrite oxidation: Unravelling complex magnetizations in Neogene marine sediments from New Zealand, *Earth Planet. Sci. Lett.*, *241*, 119–137, doi:10.1016/j.epsl.2005.10.017.
- Rowan, C. J., A. P. Roberts, and G. J. Rait (2005), Relocation of the tectonic boundary between the Raukumara and Wairoa domains (East Coast, North Island, New Zealand): Implications for the rotation history of the Hikurangi margin, *N. Z. J. Geol. Geophys.*, *48*, 185–196.
- Sagnotti, L., A. P. Roberts, R. Weaver, K. L. Verosub, F. Florindo, C. R. Pike, T. Clayton, and G. S. Wilson (2005), Apparent magnetic polarity reversals due to remagnetization resulting from late diagenetic growth of greigite from siderite, *Geophys. J. Int.*, *160*, 89–100, doi:10.1111/j.1365-246X.2005.02485.x.
- Smith, E. G. C., T. Stern, and M. Reyners (1989), Subduction and back-arc activity at the Hikurangi convergent margin, New Zealand, *Pure Appl. Geophys.*, *129*, 203–231.
- Smith, W. H. F., and D. T. Sandwell (1997), Global sea floor topography from satellite altimetry and ship depth soundings, *Science*, *277*, 1956–1962.
- Spörli, K. B. (1982), Review of paleo-strain/stress directions in Northland, New Zealand, and of the structure of the Northland Allochthon, *Tectonophysics*, *87*, 25–36.
- Stern, T. A. (1987), Asymmetric back-arc spreading, heat flux and structure associated with the Central Volcanic Region of New Zealand, *Earth Planet. Sci. Lett.*, *85*, 265–276.
- Stern, T. A., W. R. Stratford, and M. L. Salmon (2006), Subduction evolution and mantle dynamics at a continental margin: Central North Island, New Zealand, *Rev. Geophys.*, *44*, RG4002, doi:10.1029/2005RG000171.
- Stoneley, R. (1968), A lower Tertiary décollement of the East Coast, North Island, New Zealand, *N. Z. J. Geol. Geophys.*, *11*, 128–156.
- Sutherland, R. (1999a), Cenozoic bending of New Zealand basement terranes and Alpine Fault displacement: A brief review, *N. Z. J. Geol. Geophys.*, *42*, 295–301.
- Sutherland, R. (1999b), Basement geology and tectonic development of the greater New Zealand region: An interpretation from regional magnetic data, *Tectonophysics*, *308*, 341–362.
- Tauxe, L., and G. Watson (1994), The fold test: An eigen analysis approach, *Earth Planet. Sci. Lett.*, *122*, 331–341.
- Thornley, S. (1996), Neogene tectonics of Raukumara Peninsula, northern Hikurangi margin, New Zealand, Ph.D. thesis, Victoria Univ. of Wellington, Wellington.
- Turner, G. M. (2001), Toward an understanding of the multicomponent magnetization of uplifted marine sediments in New Zealand, *J. Geophys. Res.*, *106*, 6385–6397.
- Turner, G. M., A. P. Roberts, C. Laj, C. Kissel, A. Mazaud, S. Guitton, and D. A. Christoffel (1989), New paleomagnetic results from Blind River—Revised magnetostratigraphy and tectonic rotation of the Marlborough region, South Island, New Zealand, *N. Z. J. Geol. Geophys.*, *32*, 191–196.
- Vickery, S., and S. Lamb (1995), Large tectonic rotations since the early Miocene in a convergent plate-boundary zone, South Island, New Zealand, *Earth Planet. Sci. Lett.*, *136*, 43–59.
- Walcott, R. I. (1978), Present tectonics and late Cenozoic evolution of New Zealand, *Geophys. J. R. Astron. Soc.*, *52*, 137–164.
- Walcott, R. I. (1989), Paleomagnetically observed rotations along the Hikurangi margin of New Zealand, in *Paleomagnetic Rotations and Continental Deformation*, edited by C. Kissel and C. Laj, pp. 459–471, Kluwer, Dordrecht, Netherlands.
- Walcott, R. I., and T. C. Mumme (1982), Paleomagnetic study of the Tertiary sedimentary rocks from the East Coast of the North Island, New Zealand, *Res. Rep. 189*, 62 pp., Geophys. Div. Res., Dep. of Sci. and Ind. Res., Wellington.
- Walcott, R. I., D. A. Christoffel, and T. C. Mumme (1981), Bending within the axial tectonic belt of New Zealand in the last 9 Myr from paleomagnetic data, *Earth Planet. Sci. Lett.*, *52*, 427–434.

- Wallace, L. M., J. Beavan, R. McCaffrey, and D. Darby (2004), Subduction zone coupling and tectonic block rotations in the North Island, New Zealand, *J. Geophys. Res.*, *109*, B12406, doi:10.1029/2004JB003241.
- Wilson, C. J. N., B. F. Houghton, M. O. McWilliams, M. A. Lanphere, S. D. Weaver, and R. M. Briggs (1995), Volcanic and structural evolution of Taupo Volcanic Zone, New Zealand: A review, *J. Volcanol. Geotherm. Res.*, *68*, 1–28.
- Wood, R., and B. Davy (1994), The Hikurangi Plateau, *Mar. Geol.*, *118*, 153–173.
- Wright, I. C. (1993), Pre-spread rifting and heterogeneous volcanism in the southern Havre Trough back-arc basin, *Mar. Geol.*, *113*, 179–200.
- Wright, I. C., and R. I. Walcott (1986), Large tectonic rotation of part of New Zealand in the past 5 Ma, *Earth Planet. Sci. Lett.*, *80*, 348–352.
- 
- A. P. Roberts, School of Ocean and Earth Science, National Oceanography Centre, University of Southampton, Southampton SO14 3ZH, UK.
- C. J. Rowan, Department of Geology, University of Johannesburg, P.O. Box 524, Auckland Park 2006, Johannesburg, South Africa. (c.j.rowan@gmail.com)